The historical Greenland Climate Network (GC-Net) curated and augmented Level 1 dataset

Baptiste Vandecrux[1], Jason E. Box[1], Andreas P. Ahlstrøm[1], Signe B. Andersen[1], Nicolas Bayou[2], William T. Colgan[1], Nicolas J. Cullen[3], Robert S. Fausto[1], Dominik Haas-Artho[4], Achim Heilig[5], Derek A. Houtz[4], Penelope How[1], Ionut Iosifescu Enescu[4], Nanna B. Karlsson[1], Rebecca Kurup Buchholz[4], Kenneth D. Mankoff[6,7], Daniel McGrath[8], Noah P. Molotch[9], Bianca Perren[10], Maiken K. Revheim[1], Anja Rutishauser[1], Kevin Sampson[11], Martin Schneebeli[12], Sandy Starkweather[13,14], Simon Steffen[15], Jeff Weber[16], Patrick J. Wright[1], H. Jay Zwally[17], Konrad Steffen[4,14†]

[1]Department of Glaciology and Climate, Geological Survey of Denmark and Greenland (GEUS), Copenhagen, 1350, Denmark
[2]UNAVCO, Boulder, CO 80301, USA
[3]School of Geography, University of Otago, Dunedin, 9016, New Zealand
[4]Swiss Federal Institute for Forest, Snow and Landscape Research WSL, Birmensdorf, 8903, Switzerland
[5]Department of Earth and Environmental Sciences, Ludwig Maximilian University, Munich, 80539, Germany
[6]Autonomic Integra LLC, New York, NY 10025 USA
[7]NASA Goddard Institute for Space Studies, New York, NY 10025, USA
[8]Department of Geosciences, Colorado State University, Fort Collins, CO 80523, USA
[9]Institute of Arctic and Alpine Research, University of Colorado Boulder, Boulder, CO 80303, USA
[10]British Antarctic Survey, Cambridge, CB3 0ET, UK
[11]National Center for Atmospheric Research, Boulder, Colorado, CO 80305, USA
[12]WSL Institute for Snow and Avalanche Research SLF, Davos, 7260, Switzerland
[13]Cooperative Institute for Research in Environmental Sciences, University of Colorado Boulder, Boulder CO, 80309, USA
[14]National Oceanic and Atmospheric Administration, Boulder, CO 80305, USA
[15]Earthanme, Zürich, 8057, Switzerland
[16]Unidata Program Center, University Corporation for Atmospheric Research, Boulder, CO 80301, USA
[17]Earth System Interdisciplinary Science Center (ESSIC), University of Maryland, College Park, MD 20742, USA
†deceased

Correspondence to: Baptiste Vandecrux (bav@geus.dk)

Abstract. The Greenland Climate Network (GC-Net) consists of 31 automatic weather stations (AWS) at 30 sites across the Greenland ice sheet. The first site was initiated in 1990, and the project has operated almost continuously since 1995 under the leadership of the late Prof. Konrad Steffen. The GC-Net AWS measured air temperature, relative humidity, wind speed, atmospheric pressure, downward and reflected shortwave irradiance, net radiation, ice and firn temperatures. The majority of the GC-Net sites were located in the ice sheet accumulation area (17 AWS), while 11 AWS were located in the ablation area and two sites (three AWS) were located close to the equilibrium line altitude. Additionally, three AWS of similar design to the GC-Net AWS were installed by Prof. K. Steffen's team on the Larsen C ice shelf, Antarctica. After more than three decades of operation, the GC-Net AWS are being decommissioned and replaced by new AWS operated by the Geological Survey of Denmark and Greenland (GEUS). Therefore, making a reassessment of the historical GC-Net AWS data is necessary. We present a full reprocessing of the historical GC-Net AWS dataset with increased attention to the filtering of erroneous measurements, data correction, and derivation of additional variables: continuous surface height, instrument

40   heights, surface albedo, turbulent heat fluxes, 10 m ice and firn temperatures. This new augmented GC-Net Level 1 (L1) AWS dataset is now available at https://doi.org/10.22008/FK2/VVXGUT (Steffen et al. 2022) and will continue to be refined. The processing scripts, latest data and a data-user forum are available at https://github.com/GEUS-Glaciology-and-Climate/GC-Net-level-1-data-processing. In addition to the AWS data, a comprehensive compilation of valuable metadata is provided: maintenance reports, yearly pictures of the stations and the station positions through time. This unique dataset

45   provides more than 320 station-years of high quality atmospheric data and is available following FAIR data and code practices.

1 Introduction

1.1 Background

The Greenland Ice Sheet plays a substantial role in the global climate system. As a low-temperature topographic obstacle,

50   the ice sheet exerts important influences to regional atmospheric circulation (Bromwich et al., 1993, Hahn et al., 2020). Additionally, the majority of the ice sheet is covered with a highly reflective perennial snow cover and an overall negative net radiation budget, which makes the ice sheet a net cooling element in the global climate system (e.g. Toniazzio et al., 2004, Ridley et al., 2005). Recently, however, ice discharge via marine terminating outlet glaciers and seasonal melting of the ice sheet have both been increasing (e.g. IMBIE, 2020; Mankoff et al., 2021). This has increased the freshwater flux into

55   the North Atlantic, impacting ecosystems (e.g. Oksman et al., 2022), influencing ocean circulation (e.g. He and Clark, 2022) and contributing to global sea-level rise (Nerem et al., 2018). In spite of the development of remote sensing techniques and weather modeling, the measurement of ice sheet surface climate variables remains paramount to improving our understanding of the Greenland Ice Sheet response to climate variability.

1.2 History of the Weather Stations on the Greenland Ice Sheet

60   The Greenland Climate Network (GC-Net) of Automated Weather Stations (AWS) adds to a long history of meteorological observation on the Greenland Ice Sheet. Ice sheet meteorology began with overland expeditions during the late 19th and early 20th centuries. After the second world war, purpose-built mechanized vehicles made it possible to transport the personnel and equipment required to maintain staffed stations on the ice sheet. The British North Greenland Expedition (BNG), (1952-1954) under the leadership of C.J.W. Simpson, traversed the ice sheet in North Greenland,

65   establishing a temporary weather station at North Ice (Simpson, 1955). The contemporaneous French Expédition Glaciologique Internationale au Groenland (EGIG) was undertaken as a series of traverses between 1949 and 1967 under the leadership of Paul-Émile Victor (Finsterwalder, 1959). The larger EGIG effort included four staffed ice sheet stations: Camp IV, Camp VI, Station Centrale and Station Jarl-Joset/Dumont (Fristrup, 1962). Together, the BNG and EGIG expeditions provided some of the first reliable year-round meteorological records from the high-elevation ice sheet interior. U.S. military

70   ice sheet sites also represent a valuable source of meteorological data (Menne et al., 2012; Jensen, 2022). These include

weather stations associated with the Distant Early Warning stations DYE-2 and DYE-3 (1959-1988) and Camp Century (1960-1964).

Since the 1980's, the ice sheet summit has been a focus of automated meteorological observations. In 1987, the University of Wisconsin installed a network of eight AWS around the ice sheet summit (Steams and Weidner, 1991; Weidner and Steams, 1991; Shuman et al., 2001). These stations supported both the Greenland Ice Sheet Project II (GISP2) and Greenland Ice Core Project (GRIP), two contemporaneous deep ice-core drilling projects. This weather station network was phased out within five years. From 1991 to 1994, the Danish Meteorological Institute (DMI) operated an AWS at the GRIP-summit site. This station was moved 33 km to the GISP2 site, now known since 1997 as Summit. This DMI Summit AWS was decommissioned on 12 August 2020. DMI also operated an AWS from 1987 to 1988 on the Renland ice cap, East Greenland. The U.S. National Oceanic and Atmospheric Administration (NOAA) has also operated an independent AWS at Summit Station since 1997.

Numerous other institutions have also maintained ice sheet AWS for limited times and locations since the 1990s (e.g. Heinemann, 1999; Kendrick et al. 2018; Samimi et al., 2021; Covi et al. 2022, MacFerrin et al., 2022). Although multi-decade time-series are needed to resolve climatic trends, these short-lived AWS remain valuable to understand meteorological processes.

The Institute for Marine and Atmospheric research Utrecht (IMAU) of Utrecht University has overseen a sustained surface climate monitoring effort since 1990. Four ice sheet AWS were established upstream from the Russell Glacier near Kangerlussuaq, West Greenland (Oerlemans and Vugts 1993; van den Broeke et al., 1994; van de Wal and Russell 1994). These ice sheet AWS, designated S4, S5, S6, S9, ranged from the low ablation area at approximately 300 m above sea level (a.s.l.) to the equilibrium line at 1520 m a.s.l. A fifth AWS (S10) was installed in the lower accumulation area at 1850 m a.s.l. between 2010 and 2016. These AWS, as well as an East Greenland site in the firn aquifer region (Reijmer et al., 2019), continue to operate today.

The Japanese Meteorological Institute, in collaboration with Hokkaido University and the National Institute for Polar Research, began installing ice sheet AWS in Northwest Greenland in 2011 (Aoki et al., 2014; Matoba et al. 2015; Matoba et al., 2018). Over the following years, the Japanese Meteorological Institute installed and maintained the SIGMA-A and SIGMA-D AWS at 1490 m a.s.l. on the ice sheet, as well as the SIGMA-B AWS on the Qaanaaq ice cap at 944 m a.s.l..

The Geological Survey of Denmark and Greenland (GEUS), which was formed in 1995 from the Geological Survey of Greenland (GGU) and the Danish Geological Survey (DGU), has made on-ice glaciological and meteorological observations in Greenland since 1978. The first fully automated climate station operated between 1979-1983 near the margin of Qamanarssup Sermia (Olesen and Braithwaite, 1989). That effort was followed by other on-ice stations at Amitsuloq Ice Cap (1981-1990), and then Isortuarsuup Tasia and Paakitsup Akuliarusersua (both 1984-1987) and Storstrømmen Glacier (1989-1994; Olesen and Andreasen, 1983; Olesen and Braithwaite, 1989). In the 1990s, AWS were operated on Nioghalvfjerdsfjorden Glacier (1996-1997), Imersuaq (1999–2002), Hans Tausen Ice Cap (1994-1995), and Mittivakkat Glacier (1995-present; Thomsen et al., 1999; Reeh et al., 1999; Reeh et al.. 2001; Braithwaite et al., 1998; Konzelmann and

105 Braithwaite, 1995). In the 2000s, newer station designs were introduced and operated around Greenland (van As et al., 2009). These sites include: Narsap Sermia (2003-2006) close to Nuuk; Sermersuaq, a.k.a. Steenstrup Glacier, (2004-2008) along the Melville Bay coast (van As, 2011); Helheim Glacier in Southeast Greenland (2008-2010, Andersen et al., 2010), and Arcturus Gletscher at Malmbjerg, East Greenland (2008-2010, Citterio et al. 2009). Since 2007, GEUS has operated on-ice AWS via the Programme for Monitoring the Greenland Ice Sheet (PROMICE; http://www.promice.org), in collaboration

110 with the Technical University of Denmark (DTU) and Asiaq Greenland Survey. Between 2008 and 2010, 23 PROMICE AWS were installed in the ice sheet ablation area, with one station in the ice sheet accumulation area (Ahlstrøm et al., 2008; Fausto et al., 2021). GEUS is also involved in the GlacioBasis project, as part of the Greenland Ecosystem Monitoring (GEM) programme (https://g-e-m.dk). The GlacioBasis project has been monitoring glacier surface mass balance at the A.P. Olsen Ice Cap in East Greenland with three on-ice AWS operational since 2008 and on the Chamberlin Glacier on Disko

115 Island, West Greenland, with two AWS operating since 2015.

1.3 The Greenland Climate Network (GC-Net)

In 1990, ETH Zürich, in collaboration with GGU/GEUS, established an on-ice research camp with a meteorological tower in West Greenland, ~89 km east of Ilulissat, near the ice sheet equilibrium line (Ohmura, 1991, 1992; Greuell and Konzelmann 1994). In 1992, Konrad Steffen initiated continuous meteorology observations at this site which became informally referred

120 to as "Swiss Camp" (Steffen, 1995). In 1995, this research station became the starting point of GC-Net which expanded to include accumulation-area AWS distributed across the ice sheet. Under the NASA Program for Arctic Regional Climate Assessment (PARCA), which sought to provide the first assessment of Greenland Ice Sheet mass balance (Thomas, 2001), a network of 18 AWS were deployed with support from the U.S. National Science Foundation (NSF) (Steffen et al., 1996, Steffen and Box, 2001). Additional GC-Net sites were later added and some sites were discontinued due to logistical

125 constraints and environmental challenges.

Through the project's timespan, GC-Net accumulated 31 AWS at 30 Greenland sites (Table 1, Figure 1A). The majority of the GC-Net sites were located in the ice sheet accumulation area (17 AWS), while 11 stations operated in the ablation area. The two AWS at Swiss Camp and Petermann ELA were the only AWS at the equilibrium line altitude, although they shifted into an ablation regime in recent decades (e.g. McGrath et al., 2013). There are 16 AWS at 15 sites

130 with more than 15 years of data, 6 stations with 5-15 years of measurements, and 12 AWS that have been active less than 5 years (Table 1). The majority of the GC-Net AWS have a two-level design (Figure 1B) and six AWS are single-level "smart stake" AWS (Figure 1C), as described in Albert (2007). At Swiss Camp, meteorological observations are available for over 32 years. 16 AWS were still active in 2020 when the first AWS were decommissioned and replaced by modern AWS. All these data are contained in the GC-Net Level 1 dataset described here. The typical meteorological variables measured by the

135 GC-Net stations are: air temperature (TA), relative humidity (RH), wind speed (SW) and direction (DW), air pressure (P), downward and reflected shortwave radiation fluxes (ISWR and OSWR), net radiation flux (NR), surface height (HS) and snow, firn or ice temperatures at 10 levels (typically each meter) below the surface (TS) (Figure 1B). We also include in this

dataset three AWS of similar design as the GC-Net stations installed by K. Steffen's team on the Larsen C Ice Shelf, Antarctica and which went through the same re-processing as the GC-Net AWS data (Kuipers Munneke et al., 2017;
140 McGrath et al., 2021).

In 2020, after delivering nearly thirty years of GC-Net service, Konrad Steffen died in an accident during fieldwork at Swiss Camp. His scientific contributions to the ice sheet research community have been highlighted by Box et al. (2021). Following Steffen's tragic death, and according to a plan already initiated with him, GEUS took forward the climate monitoring at the main GC-Net sites. GEUS began maintaining and replacing individual stations in 2021, while WSL
145 compiled the GOES and Argos satellite transmissions. By 2022, the majority of the original GC-Net stations have been replaced, with the exception of the Summit and Petermann ELA AWS, which are planned to be replaced in the coming years. These new GEUS-maintained AWS, which will carry forward the name of "GC-Net", will be described in a separate publication and their data are distributed through https://promice.dk. Developing the historical GC-Net data into a quality-controlled, well-documented, open-access, FAIR product (Findable, Accessible, Interoperable and Reusable, Wilkinson et
150 al., 2016), operating seamlessly with the contemporary GEUS-era GC-Net data, is the primary motivation of the work presented here.
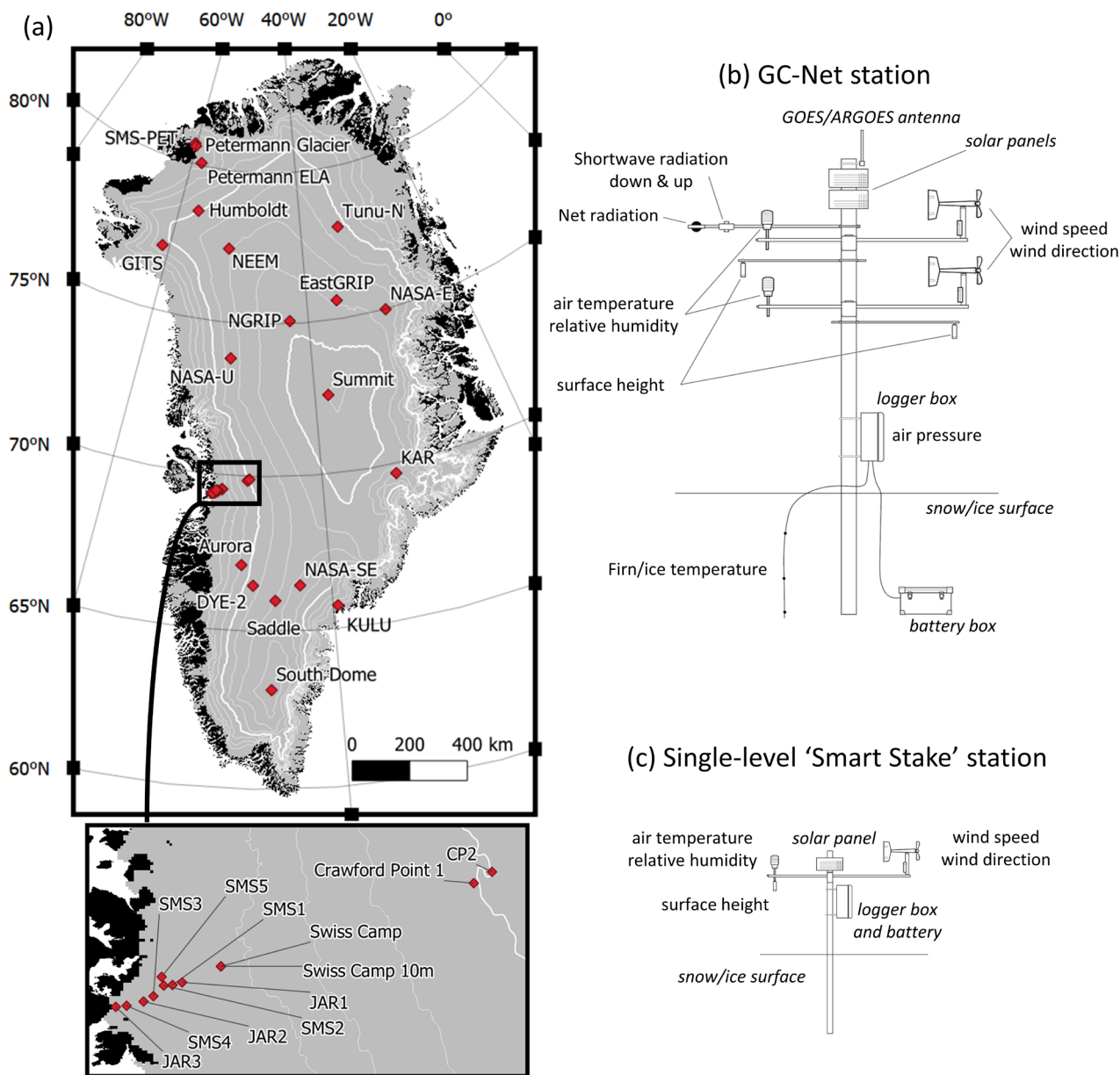
Figure 1. (a) GC-Net weather stations in Greenland. Thick white lines are 2000 and 3000 m elevation contours while thin white lines are 250 m elevation contours. (b) Design of the GC-Net weather station (two-level design). (c) Design of the single-level 'Smart Stake' station.

155

Table 1. List of the GC-Net AWS with coordinates and date of installation/decommission. The coordinates are the long-term average location or best available values. When possible, temporally resolved coordinates are also provided in the metadata.

Name	Latitude (°N)	Longitude (°E)	Elevation (wgs84 m)	Date of installation	Last valid time	Length of record (years)
Swiss Camp 10m	69.5556	-49.3647	1138	1990-05-09	2020-11-03	30.51
Swiss Camp	69.5556	-49.3647	1138	1995-01-01	2022-08-03	27.61
Crawford Point 1	69.8742	-47.0242	2022	1995-05-23	2020-07-22	25.18
NASA-U	73.8407	-49.5265	2369	1995-05-31	2022-09-20	27.33
GITS	77.1378	-61.0411	1887	1995-06-07	2021-08-13	26.20
Humboldt	78.5283	-56.8423	1950	1995-06-22	2022-06-25	27.03
Summit	72.5797	-38.5045	3254	1996-05-13	2022-09-20	26.37
Tunu-N	78.0188	-33.9668	2113	1996-05-16	2022-09-20	26.36
DYE-2	66.4820	-46.2908	2165	1996-05-24	2022-09-20	26.34
JAR1	69.4933	-49.7142	900	1996-06-19	2019-09-08	23.24
Saddle	65.9999	-44.5026	2451	1997-04-20	2021-10-16	24.51
South Dome	63.1489	-44.8175	2878	1997-04-23	2021-06-21	24.18
NASA-E	75.0023	-29.9838	2610	1997-05-03	2022-09-20	25.40
CP2	69.9133	-46.8547	1990	1997-05-12	2001-05-29	4.05
NGRIP	75.0998	-42.3326	2950	1997-07-09	2010-05-08	12.84
NASA-SE	66.4779	-42.4951	2360	1998-04-24	2019-09-26	21.44
KAR	69.6994	-33.0006	2579	1999-05-19	2001-06-07	2.05
JAR2	69.4200	-50.0575	568	1999-05-30	2013-06-16	14.06
KULU	65.7585	-39.6018	878	1999-06-17	2000-09-14	1.25
JAR3	69.3944	-50.3100	323	2000-05-28	2004-05-25	3.99
Aurora	67.1358	-47.2922	1798	2000-06-24	2001-05-06	0.87
Petermann Glacier	80.6836	-60.2931	~70	2002-06-04	2006-05-01	3.91
Petermann ELA	80.0993	-58.1497	907	2003-05-23	2022-09-20	19.34
NEEM	77.4413	-51.0999	2460	2006-03-29	2022-09-20	16.49
EastGRIP	75.6268	-35.9801	2653	2014-05-17	2022-09-20	8.35
SMS1**	69.4822	-49.8017	822	2001-01-01	2006-05-01	5.33
SMS2**	69.4778	-49.8828	727	2001-01-01	2006-05-01	5.33
SMS3**	69.4403	-49.9703	605	2001-01-01	2006-05-01	5.33
SMS4**	69.4013	-50.2108	387	2001-01-01	2003-05-01	2.33
SMS5**	69.5056	-49.9093	~762	2001-01-01	2003-05-27	2.40
LAR1*	-68.1411	-63.9519	~50	2008-12-23	2012-12-25	4.01
LAR2*	-67.5764	-63.2575	~50	2008-12-22	2011-11-15	2.90
LAR3*	-67.0317	-62.6503	~50	2009-08-10	2011-11-08	2.25
SMS-PET**	80.6033	-60.0536	~50	2002-06-01	2004-05-15	1.96

* Located on the Larsen C ice shelf in Antarctica

160   ** Single-level "smart stake" AWS

2. Network Description

The GC-Net sites were partly chosen in synergy with existing science projects or existing logistic links. The GC-Net program was formally initiated in 1995, with the installation of Swiss Camp, Crawford Point 1, NASA-U, GITS and Humboldt AWS. The Swiss Camp 10m AWS had been operating since 1990, continuously since June 1991 (Ohmura et al.,
165   1991, 1992). The NASA-U, GITS, and Humboldt stations were established in tandem with c. 500 m deep ice coring studies

sponsored by NSF and NASA (Bales et al., 2001a, 2001b; Mosley-Thompson et al., 2001, 2005). GITS (Greenland Ice Training Site) is located c. 5.5 km southeast of the Camp Century military base and ice core location, which, at the time, served as a practice 'skiway' for the US 109th Air National Guard ski-equipped LC-130H. The Crawford Point 1 station was installed upstream of Swiss Camp to represent the percolation area,extend the altitudinal profile to 2000 m, and to connect that with the Summit AWS record (McGrath et al., 2013). The precise location of Crawford Point (selected by John Crawford, Jet Propulsion Laboratory, California Institute of Technology) is the place where both ascending and descending NASA satellite orbits of interest intersected the 2000 m elevation contour. This contour was the focus of an early PARCA mass balance perimeter (Thomas et al., 2000).

170

In 1996, four AWS were installed. The Tunu-N AWS was installed in tandem with PARCA-sponsored coring where ice sheet snow accumulation exhibits a large-scale minimum (Sigl et al., 2015). The DYE-2 AWS was installed at the former military station of the same name. DYE-2 carries forward a legacy of glaciology and climatology measurements associated with the initial construction of the military station in 1959. DYE-2, later known as Camp Raven, now serves as the practice 'skiway' for the US 109th Air National Guard and is home for many other measurements (e.g. Samimi et al., 2020; MacFerrin et al., 2022). The JAR1 AWS was installed in the ablation area down-glacier from Swiss Camp. The Summit AWS was installed c. 1.4 km west of the GISP2 ice core that had been completed in 1993.

175

180

In 1997, South Dome, Saddle and NASA-E stations were installed alongside NASA-sponsored shallow ice-coring (Mosley-Thompson et al., 2001) and firn densification work (Hamilton and Whillans, 2000). The South Dome station is situated at the highest point on the ice sheet's South Dome, while Saddle station is situated at the lowest point on the main ice sheet topographic divide between Summit and South Dome. The same year, the CP2 station was installed ~8 km northeast from the Crawford Point AWS to capture surface topographic undulation-scale accumulation and climate variability. In 1997, the NGRIP AWS was installed at the site of a deep ice core drilling site (Dahl-Jensen et al., 2002). NGRIP AWS was discontinued in 2010 when the drilling was completed.

185

In 1998, NASA-SE was the last PARCA site where an AWS was installed in tandem with firn coring. In 1999, the Kangerdlugssuaq Accumulation Region (KAR) AWS was installed and the KULU AWS was installed within reach from Kulusuk airport in East Greenland. The same year, the JAR transect in the ablation area west of Swiss Camp received its second station JAR2. The KULU and KAR stations were both discontinued in 2000 and 2001 due to the challenges that represented strong winds, high snow accumulation and remoteness of East Greenland for station maintenance.

190

In 2000, the Aurora AWS was installed on the ice sheet ~150 km east of Kangerlussuaq in western Greenland in connection to an on-ice automobile test track. The AWS was discontinued in 2001 when the car testing project stopped. Also in 2000, the JAR transect received its third and lowest station JAR3. In 2002, Petermann Glacier AWS was installed on the floating tongue of Petermann Glacier in northwest Greenland and the Petermann ELA AWS was installed the following year. These two AWS aimed at documenting the ice-ocean interaction at Petermann Glacier (Rignot and Steffen, 2008). The Petermann station was discontinued due to the presence of crevasses. Crevasses and low snow accumulation are also now challenging aircraft access to Petermann ELA. In 2006, the NEEM AWS was installed in preparation of the deep drilling

195

200 project of the same name (NEEM, 2013). The NEEM AWS remained at that location after the drilling project finished and a new AWS was installed at EastGRIP in 2014 when a new deep drilling project started.

In 2001, five single-level 'smart stakes' AWS (Figure 1C) were installed in the lower ablation area of Sermeq Avannarleq glacier (Albert, 2007), neighbour of Sermeq Kujalleq (Jakobshavn isbræ). These smart stakes were serviced by snowmobile from Swiss Camp until 2003 (SMS4-5) and 2006 (SMS1-3). JAR3 was discontinued in 2004 due to the 205 upstream expansion of crevasses and JAR2 was discontinued in 2013 for similar reasons.

Three AWS were installed on the Larsen C ice shelf, Antarctica, in 2008 (Kuipers Munneke et al., 2017; McGrath et al., 2021). Given the similarities in the station design and data structure, we include these three Larsen C stations in this curated Level 1 (L1) data product version of otherwise Greenland-focused GC-Net data.

Beginning in August 2020, GEUS began maintaining the GC-Net stations at Swiss Camp and JAR1. In 2021, 210 GEUS installed its replacement AWS at Crawford Point 1, NASA-SE, South Dome, GITS, Saddle, NASA-U, NEEM and DYE-2. Existing stations were removed from the first four sites, DYE-2 was raised and serviced, and the remaining historical stations were left as they were. In 2022, DYE-2, Saddle, Humboldt, NEEM, NASA-E and Tunu-N, were visited but no maintenance was carried out apart from downloading data from the logger and raising the lower boom arm at NASA-E. Also in 2022, GEUS installed new AWS at Humboldt, NEEM, NASA-E and Tunu-N next to the original AWS. In 2023, 215 GEUS plans to visit as many sites as possible, including Petermann ELA, EastGRIP and Summit, where data from the existing GC-Net stations need to be retrieved and new GEUS AWS should be installed.

3 Station description

3.1 Station design and maintenance

The main characteristic of the GC-Net AWS is its two levels of measurements for air temperature, relative 220 humidity, wind speed and direction. In the L1 dataset, the variables labeled with "1" (e.g. TA1), as well as TA3, were measured or derived from the lower level. The variables labeled with "2" (e.g. DW2), as well as TA4, were measured or derived from the upper level. The two levels are typically placed with 1.2 m vertical separation, although other spacing was used on occasions when the station could not be raised and the lower level was at risk of getting buried by accumulating snow.

225 The most common GC-Net masts were aluminium tubes with 4" (10.16 cm) outside diameter, initially 6.4 m in length. Ablation area sites (JAR2-3, PET ELA, PET Glacier and the SMS) used a 3" (7.62 cm) mast. Both the 4" and 3" outside diameter mast tubes had 0.25" (0.635 cm) wall thickness. The masts were inserted into a c. 3.2 m deep hole from a borehole taken in firn using a core drill, or in ice using a steam or mechanical drill. The JAR1 station was the only ablation area station with the 4" (10.16 cm) outside diameter mast. The masts were raised (accumulation sites) or lowered (ablation 230 sites) using a 6 m high tripod and winch system (Figure 2); separating the upper section of the mast, inserting an extension in the case of accumulation area sites (or removing a section at ablation sites), then lowering the upper section back down onto

the base mast section. Over time, the base pipe reached a length of up to 30 m at NASA-SE. Low accumulation sites (e..g. Tunu-N, Humboldt, NASA-E) could be visited every one or two years. High accumulation sites, in particular NASA-SE and South Dome, needed annual visits to prevent burial by accumulating snow. Ablation area sites also needed frequent visits to

235 prevent the mast from melting out and the AWS from collapsing. It was not uncommon to find ablation area AWS masts leaning. Because of the initial (1995- ca. 2000) use of guy wires, differential compaction or the failure of one wire led to station tilt. When the station tilt was too critical, the mast was re-drilled (e.g. at DYE-2 in 2019 and 2021).

For information on the design of the meteorological tower and pre-1995 AWS at Swiss Camp, more details can be found in Ohmura et al. (1991, 1992) and Steffen et al. (1995, 1996).

240

Figure 2. Raising the Crawford Point 1 mast, 3 May 2005. K. Steffen (left), R. Huff (right). Photo J. Box.

3.2 Instrumentation

The standard instrumentation of the GC-Net AWS is provided in Table 2, compiled from Steffen et al. (1996), Steffen and Box (2001), Box and Steffen (2001a), Steffen et al., (2003, 2005, 2006). The primary temperature measurement

245 was a Type-E thermocouple (variables TA1 and TA2 in the L1 dataset). The CS500 (TA3 and TA4 in the L1 dataset) did not accurately measure temperatures below -40°C. While attention was made to keep the instrumentation consistent, exceptions include shifting the thermohygrometer from Vaisala INTERCAP 50YC (a.k.a. HUMICAP 180 packaged by Campbell Sci. as CS500) to the Vaisala HMP45 after ca. 1999, and from ca. 2008, switching to the Vaisala HMP155. The Swiss Camp AWS had more inconsistent air temperature and hygrometer instrumentation, as the site was used to test emerging

250 technologies, including tests of fan-aspirated temperature shields. Barometers were initially a Vaisala PTB101A, replaced in
c. 1999 with a PTB101B. The LI-COR LI-190SZ instrument measuring downward and reflected shortwave radiation and
surface albedo, is sensitive to the 0.4-0.7 μm spectral range. The REBS Q7.1 net radiation sensor is sensitive to the 0.25 - 60
μm spectral range. A domeless version 1 Kipp & Zonen NR-Lite net radiometer with spectral range of 0.2-100 μm was used
at Summit and Swiss Camp starting in ca. 2000. See Brotzge and Duchon (2000) for an intercomparison of the different
255 radiometers. The snow, firn and ice temperatures were measured by 10 type-T thermocouples inserted in the snow/firn/ice
with a 1 m spacing ranging from 1 to 10 m depth (Sampson, 2009). Most of these thermistor strings were discontinued in
2010. The surface height was measured with two SR50 sonic rangers. In the L1 dataset, these measurements are corrected
from the effect of air temperature (see Eq. 3 in from Fausto et al., 2021).

From 1995 to around 2000, the data logger was a Campbell Scientific CR10. These were replaced starting in 1999
260 with a CR10x until 2009 when CR1000 loggers were progressively introduced. The original Swiss Camp data loggers were
CR21, then CR21x running the 10 m tower until ca. 1998.

Table 2. Instrumentation overview.

Parameter	Instrument	Accuracy	Sample interval
Air temperature 1	Vaisala 50YC within a Campbell Scientific CS500	0.1 °C	60 s*, 15 s
Air temperature 2	Type-E thermocouple	0.1 °C	60 s*, 5 s
Relative Humidity	Vaisala INTERCAP 50YC Vaisala HUMICAP HMP45 or HMP155	5% < 90%, 10% > 90%	60 s
Wind speed	RM Young propeller-type Vane	0.1 m s-1	60 s*, 15 s
Wind direction	RM Young propeller-type Vane	5°	60 s
Air pressure	Vaisala PTB101B	0.1 hPa	60 min
Surface height change	Campbell Scientific SR50	1 mm	10 min
Shortwave radiation Albedo	Li Core LI-190 or 200SZ	5-15%	15 s
Net radiation	Campbell Scientific REBS Q7.1 Kipp & Zonen NR Lite2**	5-50%	15 s
Longwave radiation**	Kipp & Zonen CG4 Eppley Pyrgeometer	4-7%	1-15 s
Snow/firn/ice temperature	Type-T thermocouple	0.1 °C	15 s
Multiplexer	Campbell Scientific Am25T		
GPS time	Garmin	1 s	1 day
Solar panel	Campbell Scientific 10W or 20 W		

* sampling was changed from 60 to 15 s after 1999 for all sites except NGRIP.

** introduced at Swiss Camp and Summit in c. 2000.

265

Two data transmission systems were used by the GC-Net AWS. For sites south of 72°N, the National Oceanic and
Atmospheric Administration (NOAA) Geostationary Operational Environmental Satellites (GOES) system was used. For
sites north of 72°N, Argos transmission was used. K. Steffen found that the directional antenna for the more affordable
GOES transmission worked at the higher latitude NEEM and EastGRIP sites. These transmissions allowed near-real time

270 dissemination of the AWS data during the operation of the network. In the present dataset, data files retrieved from the loggers during site visits are used, unless only transmitted data are available.

For the instrumentation of the meteorological tower and pre-1995 AWS at Swiss Camp, more details can be found in Ohmura et al. (1991, 1992) and Steffen et al. (1995, 1996).

4 Data processing and enhancement

275 The GC-Net data has been processed with various software since its creation. From 1995 to 2004, GC-Net data concatenation of field-gathered or GOES/Argos transmissions was achieved using FORTRAN77 scripts, followed by Interactive Data Language (IDL) scripts for application of calibration constants and the filtering of outliers (Box and Steffen, 2001b). The GC-Net data processing was then migrated in 2004 to Matlab scripts (Bayou and Steffen, 2011) where the user could exclude outliers via a graphical user interface. These two approaches lacked transparency and repeatability, and were

280 conducted using commercial software. For the GEUS-led reprocessing, processing scripts are written in Python and in an open-source approach, allowing more transparency and straightforward repeatability via Git versioning (Vandecrux et al., 2023a). This re-processing could be done directly from the CR1000 logger files starting in 2009. For data collected by older loggers, the incomplete information about file headers and logger programs made it more complicated to work with these raw logger files. We therefore currently use historical files processed by J. Box from 1995 to 2005 and N. Bayou and K.

285 Steffen from 2005 to 2009 as input for our work. For the Swiss Camp 10 m meteorological tower, both logger files and historical FORTRAN processing scripts were available, so we could re-process the raw logger files and apply the same calibrations as in the historical FORTRAN programs. The key steps of our transparent and open-source re-processing framework is detailed in the following paragraphs and in Figure 3.

The re-processing of the historical GC-Net data presented here follows the FAIR principles (Wilkinson et al., 2022)
290 where i) both data, and crucial metadata, are *Findable* through this publication and through the referencing of the Dataverse on common web search platforms; ii) (meta)data are *Accessible* through an open and free data distribution platform; iii) the data are *Interoperable* as the (meta)data are distributed in non-proprietary, machine-readable format; iv) the (meta)data are *Reusable* as the data are fully described and processed in a transparent way.

4.1 Data processing, filtering and adjustments

295 Ideally, the data processing should start from unaltered logger files (the "Level 0" dataset, L0), however, because the data loggers used before 2009 have changing file formats and no header, we currently use historical, processed and calibrated files (as produced for Box and Steffen, 2001a), until the time when CR1000 data logger were introduced. To build the "Level 0 Merged" dataset (L0M, Figure 3), which is the starting point of our re-processing, we apply calibration coefficients to the available CR1000 logger files and append them to the pre-CR1000, historical processed files. The data is

300 then processed as illustrated in Figure 3. The first step is to remove periods where the sensor and/or station was not

functioning, and no valuable information could be retrieved from the data. For each station, a comma separated (CSV) "flag" file lists these erroneous periods along with the sensor they apply to. The CSV flag file also contains for each flagged period a comment field explaining the reason for flagging, and the operator who applied the flag, can be indicated. The processing script reads this station-specific flag file and discards the listed variables for the given periods.
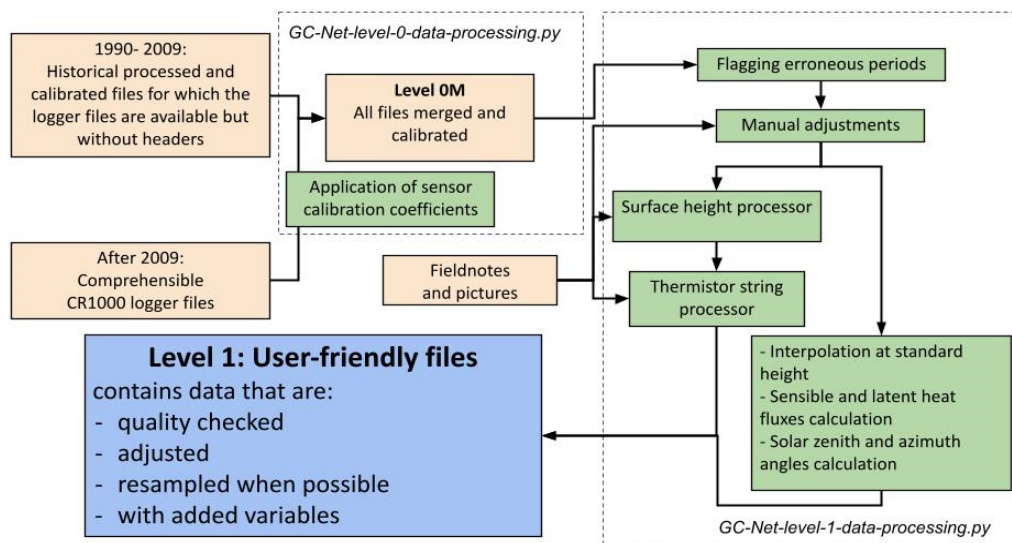
305

Figure 3. GC-Net data processing flow.

The next step adjusts the data for biases and filters noisy measurements. Filtering is done with another series of station-specific "adjustment" CSV files. Each adjustment file contains a list of time periods, variables, adjustment function name and adjustment parameters for a given station. The target variables can be passed as a list of space-separated variables

310   or as a regex (regular expression) string. The adjustment function names are self-explanatory (e.g. "add", "multiply", "rotate", "swap_with_", "min_filter, "max_filter"). The processing script then applies the given function on the listed variables during the specified period. These adjustments allow, for example, to correct for wind direction installed with an offset of 180°, therefore giving rotated wind direction, adjust for a shift in air pressure due to a missing or changing offset in the barometer measurement, or for constructing the augmented or added variables listed in the next section (height of the

315   wind sensors, continuous surface height). A comment for each modified period reports the motivation, e.g. a reported sensor malfunction, power failure, frozen anemometer propeller, or unlikely values after comparison with an external dataset. When the suspicious data and its adjustment were discussed online on the project's issue page (https://github.com/GEUS-Glaciology-and-Climate/GC-Net-level-1-data-processing/issues), the URL to the discussion is given in the comment field of the flagging or adjustment file. Attention was given to harmonize all relative humidity into values relative to saturation water

320   vapor pressure over water, so that they can be converted into values relative to saturation water vapor pressure over ice later in the processing script (see next section). All these adjustments were determined through the evaluation of station photos (Box et al., 2023), field notes (Vandecrux et al., 2023b), and comparisons with secondary AWS and regional climate outputs

(Vandecrux, 2023). Time shifts were applied to many stations to compensate for data logger clock drift. These time shifts were persistent at Humboldt where the logger clock was shifted by several months every year. The value of the time shift correction was chosen based on available field notes and on the comparison with the RACMO regional climate model (Noël et al., 2019).

Once the erroneous periods are removed and the adjustments applied, a last set of "standard" filters are applied: 1) a set of standard minimum and maximum filters is defined in a "filter" CSV file, first giving limits for each variable at all or some stations (time specific min/max need to be listed in the adjustment CSV file); 2) a persistent value filter that detects periods where values do not change (e.g. anemometer covered in rime), 3) the removal of non-meaningful data such as wind direction in case of low (< 0.5 m s^{-1}) wind speed, or isolated surface height measurements. The report of the data treatment is compiled in a single file available here:

https://github.com/GEUS-Glaciology-and-Climate/GC-Net-level-1-data-processing/blob/main/out/report_with_toc.md.

The idea behind the open and transparent processing of the GC-Net data is that data users can investigate the site or variable of their interest, and see what type of filtering or adjustments have been applied. Data users can post issues on the processing repository with questions or pointing at sensor malfunctions not yet removed from the data. Thereby, this transparent interaction with the data from all users can benefit all users. This flagging and adjustment framework, developed and tested on the GC-Net dataset is now also used for operational PROMICE AWS (https://github.com/GEUS-Glaciology-and-Climate/PROMICE-AWS-data-issues).

4.2 Augmented, corrected, and added variables

The GC-Net L1 dataset contains several variables that are derived or adjusted from the L0 data (e.g. instrument heights, relative humidity corrected for subfreezing conditions) and other variables that are added to the dataset to make the dataset easier to use (e.g. solar zenith and azimuth angles, time-stamped station position).

Instrument heights: Each station is equipped with two sonic rangers measuring the distance between each sensor and the surface (Table 2, Figure 1B). However, these sensors are not installed with a fixed height offset compared to the height-sensitive measurements (air temperature, relative humidity, wind speed and direction). Additionally, the offset between the sonic ranger and the other instruments changes for each station and can also change through time as the station is maintained. Consequently, the sonic ranger height from the L0 data are converted into instrument heights (HW1 and HW2) in the Level 1 dataset by a series of time specific adjustments to match the instrument height reported during station maintenance (Figure 4). The maintenance data, digitized from field books (Vandecrux et al., 2023b) are compiled in a spreadsheet also available in the metadata folder of the L1 dataset. For periods and sites where no measurements of sensor heights were reported, a photogrammetric estimation of instrument heights (Box et al., 2023a) was derived from available photos (Box et al., 2023b). In the L1 data, we made HW1 or HW2 match with the reported or estimated heights of the anemometer. On a leveled GC-Net AWS, the anemometer height should be the same as the T/RH sensors. However, on many occasions, the tilt of the station (not recorded) led to obvious differences between the reported height of the T/RH

sensor and the reported HW (Figure 4). This error is currently not accounted for in the L1 product but can be investigated through evaluation of the field books, maintenance spreadsheet and the photo archive (Box et al., 2023b).
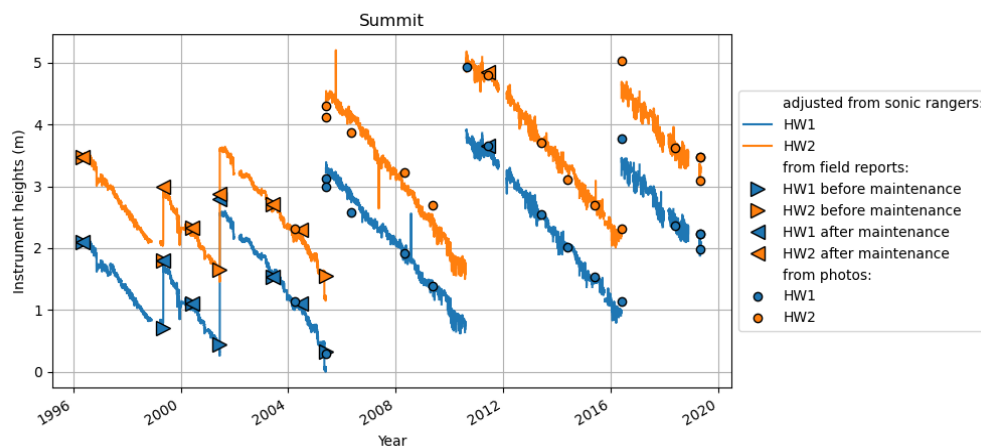
Figure 4. Instrument heights for the Summit AWS. Triangles are instrument heights measured by operators in the field (pointing
360 **right: before maintenance, pointing left: after maintenance) while the dots are heights estimated from field pictures.**

Continuous surface height: The raw sonic ranger heights (HW1 and HW2 in the L0 dataset) and the height of the instruments (HW1 and HW2 in the L1 dataset) include jumps whenever the station, or an instrument was shifted up or down. We reconstruct a continuous surface height (HS1 and HS2 in the L1 dataset) by removing all these jumps in HW1 and HW2. The results at different stations appear in Figures 4 and 5. The zero-height reference is arbitrarily set to the first recorded
365 value. In cases when the sonic rangers were failing, the height after the gap was adjusted so that the trend is preserved. Though, the assumption of a purely linear trend means that data users should consider only the continuous periods for quantitative inferences.

Relative humidity correction and specific humidity calculation: The capacitance hygrometers used on the GC-Net stations respond to relative humidity with respect to water. Thus, under sub-freezing conditions, Goff-Gratch equations (Goff
370 and Gratch 1946) are used to calculate the corrected relative humidity (RH1_cor and RH2_cor in the L1 dataset) with respect to ice (Anderson, 1994, 1995). These corrected RH are then converted into specific humidity (Q1 and Q2 in the L1 dataset). Relative correction and specific humidity calculation are done following the same scheme used for PROMICE AWS data (Fausto et al., 2021) now available through the *pypromice* python package (How et al., 2022).

Net radiation corrected from wind effect: The observations from both REBS Q7.1 and Kipp & Zonen NR-Lite
375 instruments are corrected for the effect of wind as specified by the manufacturers (Campbell Scientific, n.d.; Kipp & Zonen, n.d.). The corrected values are available under the NR_cor in the L1 dataset.
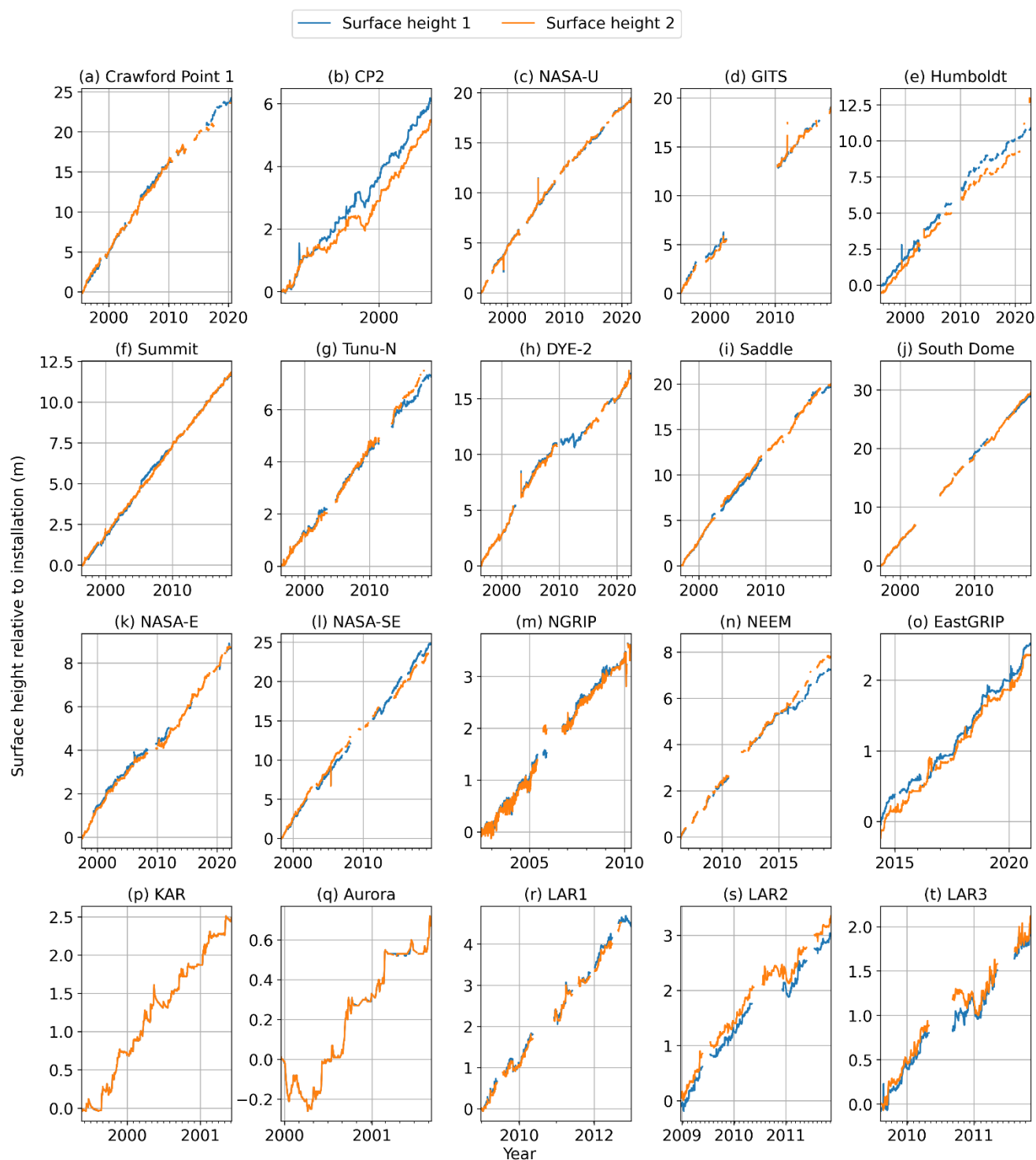
Figure 5. Overview of the reconstructed surface height for the GC-Net sites located in accumulation regions.
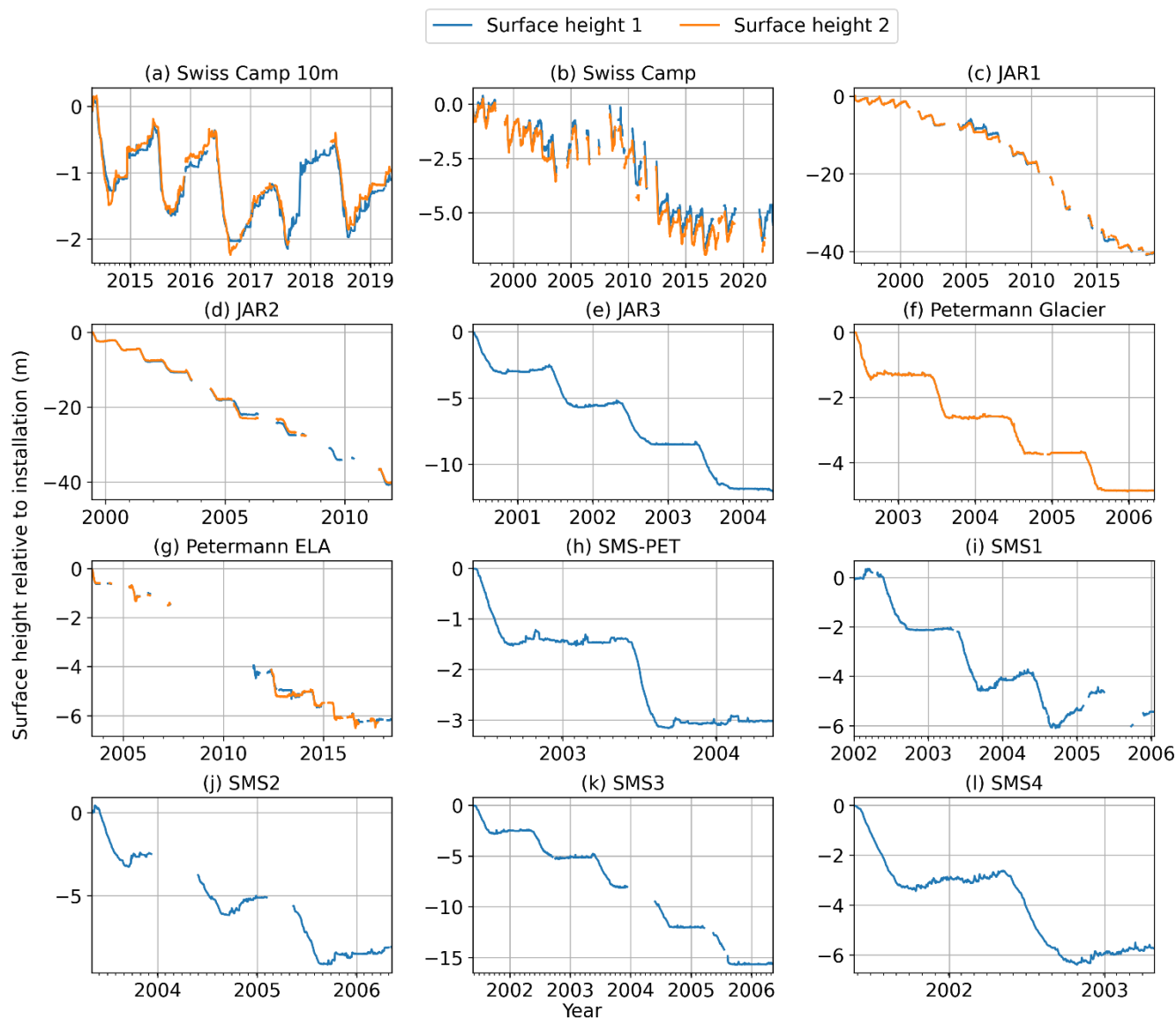
Figure 6. Same as Figure 5, but to ablation area sites.

Solar zenith and azimuth angles: The solar azimuth (SAA) and zenith angles (SZA) are key variables when using the irradiance data from the GC-Net AWS. We calculate, for each station location, SZA and SAA using the *pypromice* python package (How et al., 2022).

Surface albedo: The surface albedo is calculated from hourly averages as the ratio of the reflected to downward shortwave irradiance. Hours with SZA > 70 °, low illumination conditions (ISWR or OSWR < 100 m W^{-2}) and impossible albedo values (<=0 or >=1) are discarded. The calculated albedo is very sensitive to instrument level and periods with frost

obscuring one or both of the pyranometers. We therefore advise to use the more robust daily average albedo values, or a running hourly integration of daily values such as presented in van den Broeke et al. (2004); Stroeve et al (2013). We recommend caution when using the hourly albedo values until further assessment and correction of pyranometer sensor tilt is made. See Section 5.4 Dataset evaluation and known limitations for more detailed information.

Air temperature, relative humidity and wind speed at standardized height: The inter/extrapolation of air temperature, relative humidity and wind speed at 2, 2, and 10 m respectively is performed linearly from the two levels.

Turbulent heat fluxes: The purpose of the two levels on the GC-Net AWS is to capture the near-surface gradients in T, RH and VW, and to derive the turbulent sensible and latent heat fluxes resulting from these gradients (e.g., Box and Steffen, 2001; Cullen et al., 2014). The sensible and latent heat fluxes (SHF and LHF) are calculated using the method from Steffen and DeMaria (1996) as coded in the *JAWS* python package (Zender et al., 2018). SHF and LHF calculations are sensitive to data quality and accuracy of the instrument heights (Box and Steffen, 2001a) and should be used with caution.

Depth of the thermistor strings and 10 m ice/firn temperature: The GC-Net AWS monitor snow, ice and firn temperatures through 10 thermistors (Figure 1B). The depth of each thermistor (DTS1-10 in the L1 dataset) is estimated for each time step from the available installation depth reported in field books and from the continuous surface height following a similar procedure as Vandecrux et al. (2020). While, Vandecrux et al. (2020) found that on the first year following the installation, firn compaction reduces the spacing by c. 15% near the surface and c. 3% down to 10 m depth, compaction of the firn between the sensors is not accounted for in the L1 dataset. The ice or firn temperature at a standardized 10 m depth (TS_10m in the L1 dataset) below the surface is linearly inter- or extrapolated from the available measurements with the condition that at least one sensor is located within ± 1.5 m from the 10 m depth.

Station position through time: Over the three decades of measurements, the ice on which the GC-Net AWS are standing has been advected towards the ice sheet margin due to ice flow. We compiled all the available GPS measurements to document the AWS displacements (Vandecrux and Box, 2023c). For the stations located in areas of faster ice flow (Swiss Camp, Crawford Point 1, NASA-U, GITS, Tunu-N, DYE-2, JAR1, NASA-E, NASA-SE and Petermann-ELA) and when sufficient GPS measurements are available, we inter- or extrapolate the hourly position of the station by fitting a first order spline to the observed coordinates. These inter- or extrapolated coordinates are available in L1 data files as "Lat" and "Lon". The interpolation is done using a spline best fit and is therefore not exactly matching observations when available but rather looking at the trend in sets of observed coordinates. This approach was more robust to inaccuracies in some of the handheld GPS positions. For the remaining stations (not moving or insufficient GPS measurements), the coordinates from Table 1 are included in the "Lat" and "Lon" variables in the L1 data files. An example of these measured and inter/extrapolated annual coordinates is given in Figure 7 for JAR1 AWS.
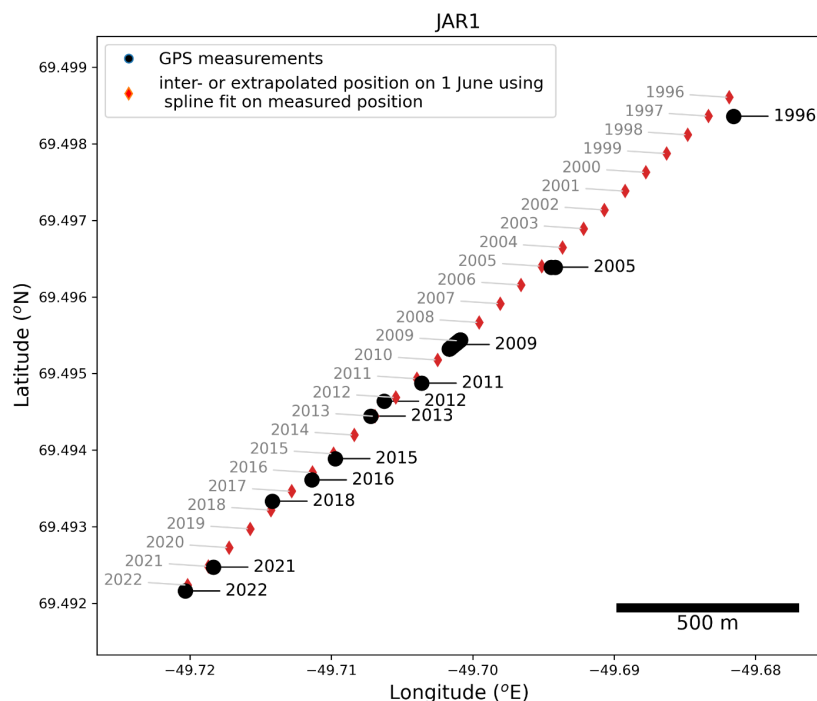
Figure 7. Example of handheld GPS observations of JAR1 AWS position (black dots) and interpolation to annual position using a
spline fit of the observations (red diamonds).

5 Dataset overview

5.1 Format and structure

The GC-Net Level 1 dataset is made available in Non-binary Environmental Archive Date (NEAD) format, which is a csv file with an added metadata header. The format is described in Iosifescu Enescu et al. (2020) and the pyNEAD python package (Mankoff and Vandecrux, 2023) is used to read and write NEAD files. The GC-Net Level 1 dataset contains both hourly and daily values in their respective folders, and, respecting the historical distribution of GC-Net data, the time stamp was set to the end of the measurement interval and documented accordingly in the NEAD file header. The data is divided into a folder for hourly averages and a folder for daily averages. A ReadMe file, as well as csv files listing the AWS reference coordinates and the variables contained in the L1 dataset are available in the dataset root directory. The compilations of maintenance reports from the AWS are available at Vandecrux et al. (2023b), the field picture archive is stored at Box et al. (2023b) and the collection observed GPS coordinates is available at Vandecrux et al. (2023c).
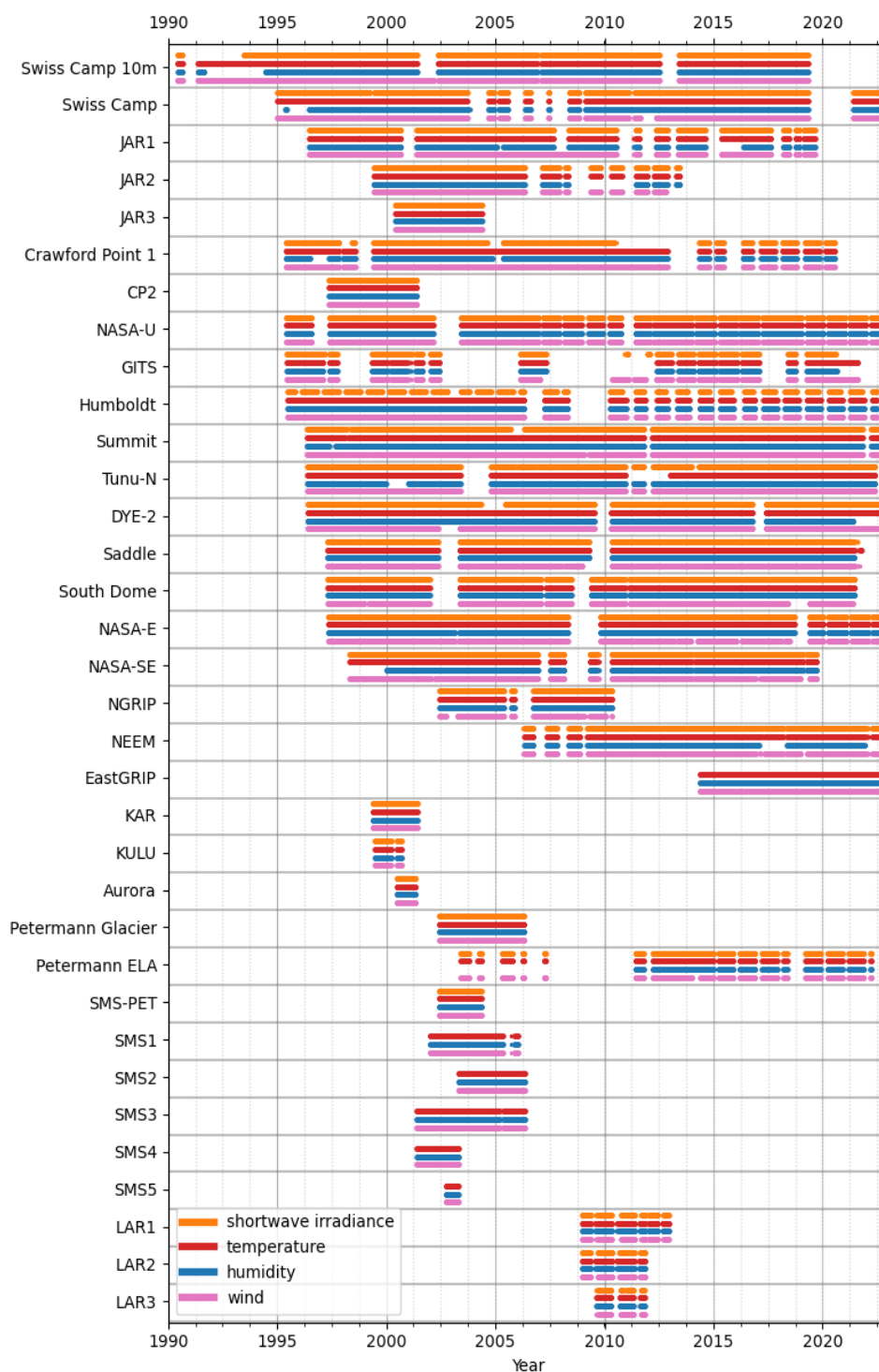
Figure 8. Data availability for shortwave irradiance, air temperature, humidity and wind speed/direction data.

5.2 Data coverage

435 Operating a weather station on the Greenland ice sheet is a technical and logistical challenge. The instrumentation, power management and data storage strategies were designed to withstand these harsh conditions. Yet many issues were reported through the years and these failures include among others: power shortage or short circuits (e.g. repeatedly at GITS), cables being pulled due to snow compaction, AWS getting buried when site visits were not made, AWS in the ablation area melting out and collapsing (mainly JAR1-3 and SWC AWS), logger clock malfunction (e.g. repeatedly at Humboldt), or individual

440 sensor failure due to extremely low temperatures, rime or liquid water. An overview of the data availability for the four main variables (shortwave irradiance, air temperature, humidity and wind speed/direction) is provided in Figure 8.

Table 3. Seasonal average near surface air temperature as calculated from the climatology presented in Figure 9.

Site	Average near surface air temperature (°C)				
	Winter	Spring	Summer	Autumn	Year
Swiss Camp	-20.1	-14.4	-0.5	-12.2	-11.8
Crawford Point 1	-26.5	-20.2	-5.7	-19.4	-17.9
NASA-U	-33	-25	-8.9	-24.7	-22.9
GITS	-33.2	-25.8	-7.7	-23.6	-22.5
Humboldt	-36.5	-28.1	-8.4	-26.8	-24.9
Summit	-38.6	-30.8	-14.2	-31.1	-28.6
Tunu-N	-38.5	-29.9	-10	-29.8	-27
DYE-2	-27.2	-19.6	-5.4	-18.2	-17.6
JAR1	-18	-12.6	0.6	-10.4	-10.1
Saddle	-29	-21.2	-7.4	-20.8	-19.6
South Dome	-28.2	-20.5	-8.6	-19.8	-19.3
NASA-E	-38	-29.5	-12.2	-29.5	-27.3
NASA-SE	-28.8	-21.4	-8	-20.9	-19.8
Petermann ELA	-28.6	-20.7	-1.2	-18.2	-13.7
NEEM	-37.7	-29.4	-10.9	-29.4	-26.8
EastGRIP	-41.6	-30.6	-12.4	-30.5	-28.7

5.3 Climatology at the GC-Net sites

445 The GC-Net weather stations are located primarily in the higher elevation accumulation zone of the ice sheet, with near-surface air temperature remaining below freezing year round (Figure 9) and annually increasing surface heights due to snow accumulation (compensated by the ice sheet motion, which is not measured by the AWS). The lowest average temperatures are found at Summit station (Table 3), at the topographic high point of the ice sheet (3254 m a.s.l.). The Swiss

Camp, JAR and Petermann stations, which represent relatively higher temperatures at or below the equilibrium-line altitude

450   (ELA), are characterized by above-freezing summer air temperatures (Table 3) and net annual ablation (loss in surface height).

All sites exhibit a distinct summer season between DOY 100-300, characterized by a peak in near-surface air temperature during the warmest month of July (Figure 9). When compared to the winter season, the summer season shows lower variability in near-surface air temperature and relatively low wind speeds (Figure 9 and 10). The winter season is

455   characterized by a prolonged period of consistently lower temperatures and higher winds spanning December through February (Figure 9 and 10).

Many GC-Net stations are approaching a climatologically significant period of record (~30 years), providing valuable records of long-term trends in both air temperature and surface-height change.
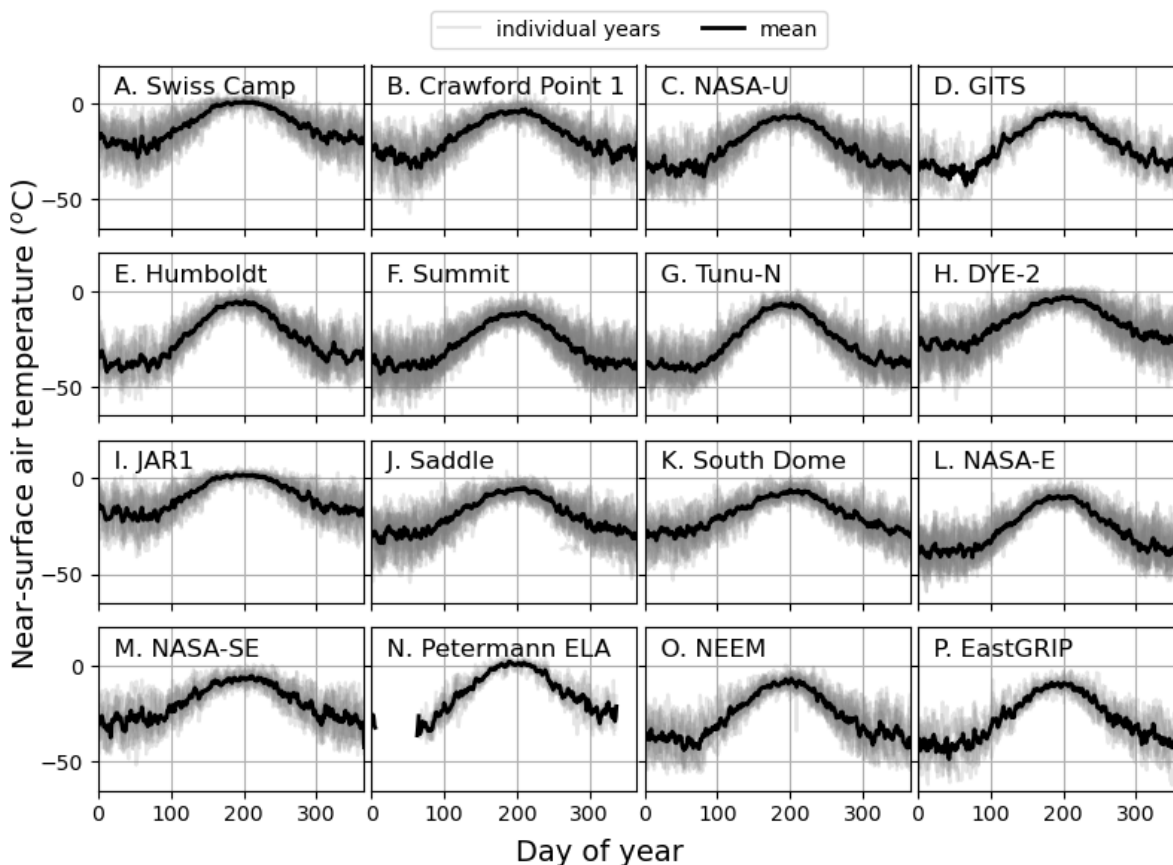
460   **Figure 9: Climatology of daily near-surface air temperatures. The interpolated 2 m air temperature is used when the two levels are available, otherwise a single measurement level is used.**
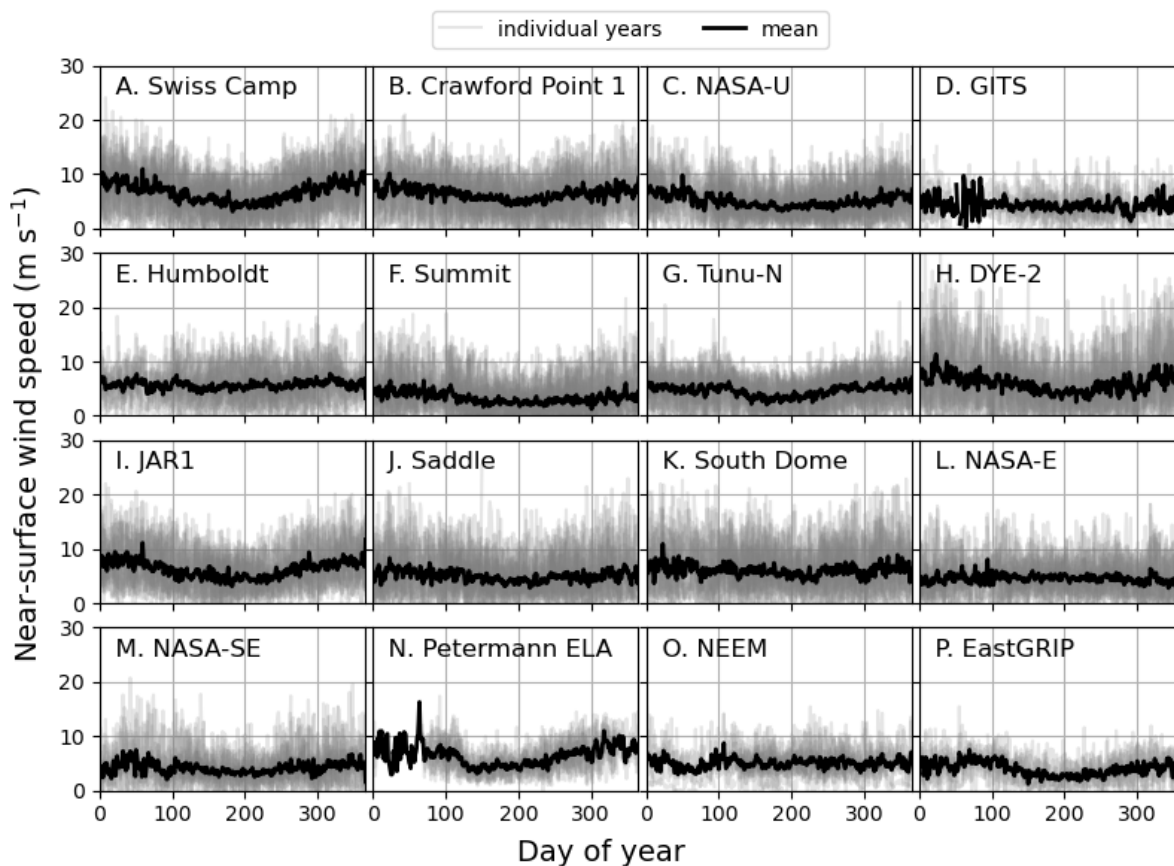
Figure 10: Climatology of the near-surface wind speed. An extrapolated 10 m wind speed is used when the two levels are available,
465 **otherwise the available level is used.**

5.4 Dataset evaluation and known limitations

With the longevity of some stations (e.g. more than 30 years at Swiss Camp), questions can be raised about the quality and accuracy of the sensors that have been deployed for several years, i.e. sensor drift and deterioration. We here evaluate the air temperature, relative humidity, wind speed, downward and upward shortwave irradiance at nine GC-Net sites relative to

470 independent AWS data during the 2007-2022 period. At Swiss Camp, NASA-E, NASA-U, NEEM, Saddle and DYE-2, the GC-Net data are compared, respectively, to measurements from the SWC, NAE, NAU, NEM AWS installed by GEUS within 500 m of the GC-Net stations. DYE-2 data are also compared to measurements from Samimi et al. (2022). The GC-Net station at Summit is compared to the nearby (within 2 km) DMI and NOAA measurements. The metrics presented in Table 4 can be considered as the overall assessment of the relative accuracy and a conservative measurement for the

475 repeatability of the GC-Net data.

Table 4. Comparison of the GC-Net AWS data to independent AWS observations at the GC-Net sites. ME stands for mean error and RMSE for root mean squared error.

GC-Net AWS	Secondary AWS	ME	RMSE	GC-Net AWS	Secondary AWS	ME	RMSE	GC-Net AWS	Secondary AWS	ME	RMSE
Downward shortwave irradiance (W m⁻²)				*Air temperature lower (ºC)*				*Relative humidity upper (%)*			
Swiss Camp	SWC	-7.8	41.4	NASA-E	NAE	-0.2	1	NASA-U	NAU	-0.8	3.6
NASA-U	NAU	-21.2	44	Summit	NOAA	0.5	2.7	NASA-E	NAE	-3.2	4.7
NASA-E	NAE	-21	35.6	*Air temperature upper (ºC)*				*Wind speed lower (ms⁻¹)*			
NEEM	NEM	-28.6	52.9	Swiss Camp	SWC	0	0.4	NASA-U	NAU	-1.2	1.4
Saddle	SDL	-0.3	60.7	NASA-E	NAE	-0.2	1.1	NASA-E	NAE	-5.5	5.6
DYE-2	U. Calgary	-17.9	60.3	EastGRIP	EGP	0.1	0.6	NEEM	NEM	-1.9	2.3
DYE-2	DY2	-6.3	29.5	Summit	DMI	0.7	2.3	DYE-2	DY2	-0.2	0.9
Reflected shortwave irradiance (W m⁻²)				Summit	NOAA	-2	4	*Wind speed upper (ms⁻¹)*			
Swiss Camp	SWC	-7.3	27.4	*Surface pressure (hPa)*				Swiss Camp	SWC	0.4	0.7
NASA-U	NAU	-1.4	16.9	Swiss Camp	SWC	3.4	4	NASA-U	NAU	-0.4	1
NASA-E	NAE	-24.4	35	NASA-U	NAU	-10.6	14	NASA-E	NAE	-1.6	1.9
NEEM	NEM	-9.9	16.7	NASA-E	NAE	0.7	0.8	EastGRIP	EGP	-0.3	0.8
Saddle	SDL	12.2	47	EastGRIP	EGP	0.7	1.7	Saddle	SDL	-1.1	2.4
DYE-2	U. Calgary	-5.8	33.7	Saddle	SDL	-0.3	0.6	Summit	DMI	0.8	2.4
DYE-2	DY2	-13.2	24.9	DYE-2	U. Calgary	-0.3	0.5	Summit	NOAA	-1.6	2.5
Albedo (-)				Summit	NOAA	0.5	5.3	*Wind direction lower (º)*			
Swiss Camp	SWC	0	0.06	*Relative humidity lower (%)*				NASA-U	NAU	-47.9	61.7
NASA-U	NAU	0.1	0.11	Swiss Camp	SWC	8.1	8.8	NEEM	NEM	6.4	45.5
NASA-E	NAE	-0.02	0.03	NASA-U	NAU	-1.7	4.2	DYE-2	DY2	-4	37.7
NEEM	NEM	0.03	0.07	NASA-E	NAE	-2.7	5.2				
Saddle	SDL	0.03	0.11	EastGRIP	EGP	-9.5	11.1				
DYE-2	U. Calgary	0.01	0.08	DYE-2	U. Calgary	1.7	2.5				
DYE-2	DY2	-0.04	0.06	Summit	DMI	-1.5	5.4				
				Summit	NOAA	-4.4	7.9				

480   Some of the discrepancies between the different AWS measurements in Table 4 are likely due to known limitations of the GC-Net AWS instruments. The GC-Net air temperature measurements were "naturally aspirated", i.e. not ventilated using motorized fans, and therefore subject to solar overheating under low wind speed and high shortwave irradiance (Steffen and Box, 2001; Box and Steffen, 2001a). However, by comparing the GC-Net measurements to the air temperatures values from actively ventilated instruments on the newer AWS installed at the GC-Net sites (Table 4), we found that this

485   effect can be very site-specific. When comparing 12 collocated pairs of ventilated and unventilated instruments in low wind speed conditions (<2 m s^{-1}) and high downward shortwave irradiance (>200 W m^{-2}), linear correlation between unventilated-to-ventilated temperature difference and downward shortwave irradiance was significant ($P<0.05$) in a minority of 4 cases, while the remaining 8 comparisons had insignificant control of downward irradiance on the temperature difference.

        The hygrometers are sensitive to the harsh conditions on the ice sheet and prone to degradation. Ohmura et al.

490   (1991, 1992) also noted issues with the absolute calibration of the hygrometers installed at Swiss Camp in 1990-1993. The main limitations of hygrometers are their inability to measure supersaturation and the clogging of the porous sensor when the ambient air is saturated or supersaturated, and slow de-clogging when conditions are dry again (Anderson, 1995). Data quality can be judged visually from RH time series, especially in dry and windy regions: the reading will remain constant at 100% with regards to ice and then suddenly dip to more realistic drier values.

495   The downward and reflected shortwave irradiance measurements, as well as the albedo derived from them, are known to be sensitive to the leveling of the instrument (Wang et al., 2016) and the surface slope (Weiser et al., 2016; Picard et al., 2020). Apart from photogrammetric assessments, which are challenging and from very limited field notes, the tilt of the GC-Net AWS was not measured over the years. Wang et al. (2016) presented the Retrospective, Iterative, Geometry-Based (RIGB) tilt-correction method that estimates the tilt of the station from its measurement of downward shortwave

500   irradiance during clear sky days. Unfortunately, the resource files required by this algorithm (the theoretical downward shortwave irradiance to which the measurements are to be compared) were discontinued after 2015. We have begun working on applying the method to the GC-Net data as part of a future release. Until this correction has been applied, we advise caution when using the radiation and albedo data.

        The shortwave irradiance and wind speed measurements are subject to the shadowing of the station. The former

505   when the station's shadow passes over the sensor, for the latter when the anemometer is downwind of the station. These issues were minimized through the design of the station, by installing the pyranometer boom directed south or the anemometers across from the predominant wind direction. Additionally, under certain conditions (e.g., station standing high above the surface), the station mast and logger box may enter the field of view of the pyranometer. Consequently, the AWS may mask part of the diffuse irradiance from the snow. This effect can be corrected, for example on the albedo values in

510   Eq.16 of Aoki et al. (2011), but the exact geometry and tilt of the station is required. This is not pursued here but may be in future data releases.

The type-T thermocouples measuring snow and ice temperature are subject to noise (Cathles et al., 2007, Sampson, 2009). The cause is the reference temperature in the data logger enclosure being insufficiently stable. These data should therefore be used with caution.

515   Through this review of potential measurement errors, we do our best to highlight potential issues to the data users, especially for applications highly sensitive to data quality. Nevertheless, these errors should be punctual and the majority of the record can be considered as a robust measurement of the surface climate within the uncertainty linked to the sensors (Table 2) and the practical uncertainty found through comparison with other AWS (Table 4).

6 Concluding remarks

520   The Level 1 reprocessing of the historical GC-Net AWS data brings the GC-Net data to a higher quality standard, distributed under the *FAIR* principles (Wilkinson et al., 2022). This ultimately paves the way to merging these records with data from the modern GC-Net AWS installed by GEUS at the GC-Net sites since 2021. In addition to the iterative procedure of identification and removal of residual erroneous data through an inclusive community effort via the Github issues page, future work is to focus on establishing solar irradiance tilt correction and the study of the long-term effect of firn 525 densification on surface height records.

       The GC-Net AWS represent the most widespread and longest consistent meteorological dataset on the Greenland ice sheet, with the monitoring sites having reached, or approaching, a climatologically significant time span. The GC-Net data can be used for long-term climate evaluation, but also for process-oriented studies, as ground truth for remote sensing products and regional climate models. These datasets are therefore an essential and valuable asset to assess the response of 530 the Greenland ice sheet to a changing climate.

Data and code availability

       The stable version of the GC-Net Level 1 dataset is available at https://doi.org/10.22008/FK2/VVXGUT (Steffen et al., 2022). Although many of the AWS have been discontinued, the Level 1 dataset is to be refined through an iterative process of identification and removal of spurious data and potential adjustments of measurements. Updates, i.e. the latest and 535 most refined data are available on the GC-Net-level-1-data-processing repository (Vandecrux et al., 2020). Data users are encouraged to ask their questions and report issues on the issue page of the GC-Net-level-1-data-processing repository. The maintenance reports from the AWS are available at https://doi.org/10.5281/zenodo.7829106 (Vandecrux and Box, 2023) and the fieldwork pictures sorted by site and year are available at https://doi.org/10.5281/zenodo.7839788 (Box et al., 2023b).

       The pyNEAD python package is recommended to read and write NEAD files and is archived at 540 https://doi.org/10.5281/zenodo.7728587 (Mankoff and Vandecrux, 2023). For each new release of the Level 1 dataset, the processing scripts will be captured into a code release on the GC-Net-level-1-data-processing repository (Vandecrux et al.,

Earth System
Science
Data

2020). This repository also contains diagnostic plots and codes used to produce Figure 4 and 5. The GPS coordinates inter- and extrapolation scripts, as well as the plotting code for Figure 7 are available at https://doi.org/10.5281/zenodo.7729070 (Vandecrux and Box, 2023b). The scripts used for the evaluation of the GC-Net data against independent AWS and the study

545 of the AWS climatology (Figures 7-8 and Tables 3-4) are available at https://doi.org/10.5281/zenodo.7728938 (Vandecrux, 2023).

Acknowledgments

In addition to the support from several past NASA and NSF grants awarded to K. Steffen (grant nr. NAPW-2158, NAG51-1612, NAG5-10600, NAG5-10857, NNG06GB08G, OPP-9423530), financial support of the 2020 transition came from the

550 DANCEA (Danish Cooperation for Environment in the Arctic) under the Danish Ministry of Energy, Buildings and Climate. The Danish Finance Law currently supports the GC-Net field and data activities. We acknowledge the key contributions from all the people that have participated in the GC-Net project, assisted Konrad Steffen through the years and contributed to the longevity of GC-Net. In particular, we acknowledge (in alphabetical order) the support from Robin Abbott, Waleed Abdalati, Todd Albert, Kate Daniels, Lucia Espona Pernas, Nena Griessinger, Alain Hubert, Russell Huff, Nighat Johnson-

555 Amin, Mike MacFerrin, Molly McCallister, Reza Naderpour, Atsumu Ohmura, Allan Ø. Pedersen, Thomas, Philipps, Gian-Kasper Plattner, Kim Petersen, Martin Proksch, Christian Schneeberger, Christopher Shields, Martina Særrelse, Julienne Stroeve, Benjamin Walter, Øyvind A. Winton and many others.

Author contributions

K.S. was leading the GC-Net project, securing funding, maintaining the stations and processing the data until 2020. B.V.

560 coordinated the effort for the reprocessing, compiled the data and metadata and drafted the manuscript. Substantial editing of the text was done by J.E.B., K.D.M., W.I.C., A.R., P.H.. A.P.A., R.S.F. and S.B.A. secured the funding for the visit of the GC-Net sites from 2020. D.A.H., P.H., P.J.W., K.D.M. and M.K.R. contributed to the reprocessing scripts and visualization. I.I.E., R.K.B. and D.H.-A. handled the transmitted data at WSL until 2022. D.A.H., S.Ste., D.M., N.B., N.J.C., M.S., S.Sta., A.H., B.P., J.W., J.Z., K.Sa., N.P.M. and J.E.B. accompanied and assisted K. S. in the field until 2020. N.B.K., A.R.,

565 K.D.M., W.T.C., A.P.A., P.H., B.V. and J.E.B. visited and maintained the GC-Net sites after 2020. All co-author reviewed and approved the manuscript.

Competing interests

B. Vandecrux and K.D. Mankoff are members of the editorial board of Earth System Science Data.

References

570 Albert, T.H: Assessment of glacier mass balances from small tropical glaciers to the large ice sheet of Greenland, Ph.D. Thesis, Florida State University, https://doi.org/10.22008/FK2/DQRE71, 2007.

Anderson, P. S.: A Method for Rescaling Humidity Sensors at Temperatures Well below Freezing, Journal of Atmospheric and Oceanic Technology, 11(5), 1388-1391., https://doi.org/10.1175/1520-0426(1994)011<1388:AMFRHS>2.0.CO;2, 1994.

Anderson, P. S.: Mechanism for the Behavior of Hydroactive Materials Used in Humidity Sensors, Journal of Atmospheric
575 and Oceanic Technology, 12(3), 662-667., https://doi.org/10.1175/1520-0426(1995)012<0662:MFTBOH>2.0.CO;2, 1995.

Andersen, M.L., Larsen, T.B., Nettles, M., Elosegui, P., Van As, D., Hamilton, G.S., Stearns, L.A., Davis, J.L., Ahlstrøm, A.P., de Juan, J. and Ekström, G.: Spatial and temporal melt variability at Helheim Glacier, East Greenland, and its effect on ice dynamics. Journal of Geophysical Research: Earth Surface, 115(F4). https://doi.org/10.1029/2010JF001760, 2010.

Ahlstrøm, A. P., and PROMICE project team: A new programme for monitoring the mass loss of the Greenland ice sheet.
580 GEUS Bulletin, 15, 61–64. https://doi.org/10.34194/geusb.v15.5045, 2008.

Ambach, W.: Untersuchungen zum energieumsatz in der ablationszone des grönländischen inlandeises, expedition glaciologique internationale au Groenland, vol. 4, 63.

Copenhagen, Bianco Lunos Ed., 1977a

Ambach, W.: Untersuchungen zum energieumsatz in der akkumulationszone des grönländischen inlandeises, expedition
585 glaciologique internationale au Groenland, vol. 4, 44. Copenhagen, Bianco Lunos Ed., 1977b.

Aoki, T., Matoba, S., Uetake, J., Takeuchi, N., and Motoyama, H.: Field activities of the "Snow Impurity and Glacial Microbe effects on abrupt warming in the Arctic" (SIGMA) Project in Greenland in 2011-2013. Bulletin of glaciological research, 32, 3-20, https://doi.org/10.5331/bgr.32.3, 2014.

Aoki, T.; Kuchiki, K.; Niwano, M.; Kodama, Y.; Hosaka, M.; Tanaka, T. Physically based snow albedo model for
590 calculating broadband albedos and the solar heating profile in snowpack for general circulation models. J. Geophys. Res. Atmos. 116, https://doi.org/10.1029/2010JD015507, 2011.

Bales, R. C., McConnell, J. R., Mosley-Thompson, E., and Csatho, B.: Accumulation over the Greenland ice sheet from historical and recent records, J. Geophys. Res., 106(D24), 33813– 33825, https://doi.org/10.1029/2001JD900153, 2001a.

Bales, R.C., Mosley-Thompson, E. and McConnell, J.R.: Variability of accumulation in northwest Greenland over the past
595 250 years. Geophysical Research Letters, 28(14), pp.2679-2682. https://doi.org/10.1029/2000GL011634, 2001b.

Braithwaite, R., Konzelmann, T., Marty, C., and Olesen, O.: Errors in daily ablation measurements in northern Greenland, 1993-94, and their implications for glacier climate studies. Journal of Glaciology, 44(148), 583-588. https://doi.org/10.3189/S0022143000002094, 1998.

Bayou, N. and Steffen, K.: QCheck: a Matlab package for the processing of GC-Net automated weather station data,
600 https://github.com/GEUS-Glaciology-and-Climate/GC-Net-Matlab-processing-scripts, Last access 01-03-2023, 2011.

Box, J.E. and Steffen, K.: Sublimation on the Greenland ice sheet from automated weather station observations. Journal of Geophysical Research: Atmospheres, 106(D24), pp.33965-33981, https://doi.org/10.1029/2001JD900219, 2001a.

Box, J.E. and Steffen, K.: FORTRAN and IDL processing scripts for the historical GC-Net data, https://github.com/GEUS-Glaciology-and-Climate/JEB_GC-Net, Last access 01-03-2023, 2001b

605 Box, J.E, Revheim, M, Vandecrux, B.: GCNet_photogrammetry: GC-Net weather station geometry from field picture photogrammetry (Version v1). Zenodo. https://doi.org/10.5281/zenodo.7729252, 2023a

Box, J.E., Vandecrux, B., Houtz, D., Steffen, K.: GC-Net historical photo archive, Zenodo, https://doi.org/10.5281/zenodo.7839788, 2023b

Box, J. E., Stroeve, J. C., and Abdalati, W.: Steffen K, Abdalati W and Stroeve J (1993) Climate sensitivity studies of the
610 Greenland ice sheet using satellite AVHRR, SMMR SSM/I and in situ data. Meteorology and Atmospheric Physics 51(3–4): 239–258. DOI:10.1007/bf01030497, Progress in Physical Geography: Earth and Environment, 45, 632–638, https://doi.org/10.1177/03091333211011368, 2021.

Bromwich, D. H., Robasky, F. M., Keen, R. A., and Bolzan, J. F.: Modeled Variations of Precipitation over the Greenland Ice Sheet, J. Clim., 6, 1253–1268, https://doi.org/10.1175/1520-0442(1993)006<1253:MVOPOT>2.0.CO;2, 1993.

615 Brotzge, J. A., and Duchon, C. E.: A Field Comparison among a Domeless Net Radiometer, Two Four-Component Net Radiometers, and a Domed Net Radiometer. J. Atmos. Oceanic Technol., 17, 1569–1582, https://doi.org/10.1175/1520-0426(2000)017<1569:AFCAAD>2.0.CO;2. 2000.

Campbell Scientific, Q-7.1 Net Radiometer, Instruction Manual, https://s.campbellsci.com/documents/us/manuals/q-7-1.pdf, Last access February 28 2023, n.d.

620 Cathles, L.M., Cathles, L.M. and Albert, M.R.: A physically based method for correcting temperature profile measurements made using thermocouples. Journal of Glaciology 53(181), 298–304. https://doi.org/10.3189/172756507782202892, 2007.

Citterio, M. ., Mottram, R., Hillerup Larsen, S., and Ahlstrøm, A.: Glaciological investigations at the Malmbjerg mining prospect, central East Greenland. GEUS Bulletin, 17, 73–76, https://doi.org/10.34194/geusb.v17.5018, 2009.

Covi F., Hock R., Reijmer C.H.: Challenges in modeling the energy balance and melt in the percolation zone of the
625 Greenland ice sheet. Journal of Glaciology 1–15. https://doi.org/10.1017/jog.2022.54, 2022.

Cullen, N.J., Mölg, T., Conway, J. and Steffen, K.: Assessing the role of sublimation in the dry snow zone of the Greenland ice sheet in a warming world. Journal of Geophysical Research: Atmospheres, 119(11), pp.6563-6577, https://doi.org/10.1002/2014JD021557, 2014.

Dahl-Jensen, D., Gundestrup, N., Miller, H., Watanabe, O., Johnsen, S., Steffensen, J., et al.: The NorthGRIP deep drilling
630 programme. Annals of Glaciology, 35, 1-4. https://doi.org/10.3189/172756402781817275, 2002.

Fausto, R. S., van As, D., Mankoff, K. D., Vandecrux, B., Citterio, M., Ahlstrøm, A. P., Andersen, S. B., Colgan, W., Karlsson, N. B., Kjeldsen, K. K., Korsgaard, N. J., Larsen, S. H., Nielsen, S., Pedersen, A. Ø., Shields, C. L., Solgaard, A. M., and Box, J. E.: Programme for Monitoring of the Greenland Ice Sheet (PROMICE) automatic weather station data, Earth Syst. Sci. Data, 13, 3819–3845, https://doi.org/10.5194/essd-13-3819-2021, 2021.

635   Goff, J. A. and Gratch, S.: Low-pressure properties of water-from 160 to 212 °F., Trans. Am. Heat. Vent. Eng., 52, 95–121, 1946.

Greuell, W. and Konzelmann, T.: Numerical modelling of the energy balance and the englacial temperature of the Greenland Ice Sheet. Calculations for the ETH-Camp location (West Greenland, 1155 m asl). Global and Planetary change, 9(1-2), pp.91-114. https://doi.org/10.1016/0921-8181(94)90010-8, 1994.

640   Hahn, L. C., Storelvmo, T., Hofer, S., Parfitt, R., and Ummenhofer, C. C.: Importance of orography for Greenland cloud and melt response to atmospheric blocking, J. Clim., 33, 4187–4206, https://doi.org/10.1175/jcli-d-19-0527.1, 2020.

Hamilton, G. S., and Whillans, I. M.: Point measurements of mass balance of the Greenland Ice Sheet using precision vertical Global Positioning System (GPS) surveys, J. Geophys. Res., 105(B7), 16295– 16301, https://doi.org/10.1029/2000JB900102, 2000.

645   He, F., Clark, P.U.: Freshwater forcing of the Atlantic Meridional Overturning Circulation revisited. Nat. Clim. Chang. 12, 449–454, https://doi.org/10.1038/s41558-022-01328-2, 2022.

Heinemann, G.: The KABEG'97 field experiment: An aircraft-based study of katabatic wind dynamics over the Greenland ice sheet. Boundary Layer Meteorol 93: 75-116, http://doi.org/10.1023/A:1002009530877, 1999.

How, P., mankoff, K.D., Wright, P.J., Vandecrux, B.: pypromice, GEUS Dataverse, V1, 650   https://doi.org/10.22008/FK2/3TSBF0, 2022.

The IMBIE Team: Mass balance of the Greenland Ice Sheet from 1992 to 2018. Nature 579, 233–239, https://doi.org/10.1038/s41586-019-1855-2, 2020.

Iosifescu Enescu, I.; Bavay, M.; Mankoff, K. Non-Binary Environmental Archive Data (NEAD) format. EnviDat, https://www.doi.org/10.16904/envidat.187, 2020.

655   Jensen, C.D.: Weather Observations from Greenland 1958-2021 - Observational Data with Description, DMI Report 22-08, https://www.dmi.dk/fileadmin/Rapporter/2022/DMIRep22-08.pdf, 2022.

Kendrick, A. K., Schroeder, D. M., Chu, W., Young, T. J., Christoffersen, P., Todd, J., et al.: Surface meltwater impounded by seasonal englacial storage in West Greenland. Geophysical Research Letters, 45, 10,474– 10,481. https://doi.org/10.1029/2018GL079787, 2018.

660   Kipp & Zonen, NR Lite 2 Net Radiometer Instruction Sheet, https://www.kippzonen.com/Download/335/Instruction-Sheet-Net-Radiometers-NR-Lite2, Last accessed 28-02-2023, n.d.

Konzelmann, T., and Braithwaite, R.: Variations of ablation, albedo and energy balance at the margin of the Greenland ice sheet, Kronprins Christian Land, eastern north Greenland. Journal of Glaciology, 41(137), 174-182. https://doi.org/10.3189/S002214300001786X, 1995.

665   Kuipers Munneke, P., McGrath, D., Medley, B., Luckman, A., Bevan, S., Kulessa, B., Jansen, D., Booth, A., Smeets, P., Hubbard, B., Ashmore, D., Van den Broeke, M., Sevestre, H., Steffen, K., Shepherd, A., and Gourmelen, N.: Observationally constrained surface mass balance of Larsen C ice shelf, Antarctica, The Cryosphere, 11, 2411–2426, https://doi.org/10.5194/tc-11-2411-2017, 2017.

LI-COR, LI-190SZ Instruction manual, https://www.fondriest.com/pdf/li-cor_190_200_manual.pdf, Last access 01-03-2023, n.d.

Finsterwalder, R.: Expédition Glaciologique Internationale Au Groenland 1957–60 (E.G.I.G.), J. Glaciol., 3, 542–546, https://doi.org/10.3189/S0022143000017299, 1959.

Fristrup, B.: Overvintringsstationer på indlandsisen - III. Amerikanske permanente stationer m.v, Tidsskriftet Grønland, ?, 321–344, 1962.

Matoba, S., Motoyama, H., Fujita, K., Yamasaki, T., Minowa, M., Onuma, Y., Komuro, Y., Aoki, T., Yamaguchi, S., Sugiyama, S., and Enomoto, H.: Glaciological and meteorological observations at the SIGMA-D site, northwestern Greenland Ice Sheet. Bulletin of glaciological research, 33, 7-14, http://doi.org/10.5331/bgr.33.7, 2015.

Matoba, S., Niwano, M., Tanikawa, T., Iizuka, Y., Yamasaki, T., Kurosaki, Y., Aoki, T., Hashimoto, A., Hosaka, M. and Sugiyama, S.: Field activities at the SIGMA-A site, northwestern Greenland Ice Sheet, 2017. Bulletin of Glaciological Research, 36, pp.15-22. https://doi.org/10.5331/bgr.18R01, 2018.

MacFerrin, M. J., Stevens, C. M., Vandecrux, B., Waddington, E. D., and Abdalati, W.: The Greenland Firn Compaction Verification and Reconnaissance (FirnCover) dataset, 2013–2019, Earth Syst. Sci. Data, 14, 955–971, https://doi.org/10.5194/essd-14-955-2022, 2022.

Mankoff, K. D., Fettweis, X., Langen, P. L., Stendel, M., Kjeldsen, K. K., Karlsson, N. B., Noël, B., van den Broeke, M. R., Solgaard, A., Colgan, W., Box, J. E., Simonsen, S. B., King, M. D., Ahlstrøm, A. P., Andersen, S. B., and Fausto, R. S.: Greenland ice sheet mass balance from 1840 through next week, Earth Syst. Sci. Data, 13, 5001–5025, https://doi.org/10.5194/essd-13-5001-2021, 2021.

Mankoff, K. and Vandecrux, B.: pyNEAD: Python interface to NEAD file format (Version v1). Zenodo. https://doi.org/10.5281/zenodo.7728587, 2023.

McGrath, D., Colgan, W., Bayou, N., Muto, A., and Steffen, K.: Recent warming at Summit, Greenland: Global context and implications, Geophys. Res. Lett., 40, 2091–2096, https://doi.org/10.1002/grl.50456, 2013.

McGrath, D., Bayou, N., and Steffen, K.: Larsen C automatic weather station data 2008–2011, U.S. Antarctic Program (USAP) Data Center. https://doi.org/10.15784/601445, 2021.

Menne, M.J., Durre, I., Vose, R.S., Gleason, B.E., and Houston, T.G.: An overview of the Global Historical Climatology Network-Daily Database. Journal of Atmospheric and Oceanic Technology, 29, 897-910, https://doi.org10.1175/JTECH-D-11-00103.1, 2012.

Mosley-Thompson, E., McConnell, J. R., Bales, R. C., Li, Z., Lin, P.-N., Steffen, K., Thompson, L. G., Edwards, R., and Bathke, D.: Local to regional-scale variability of annual net accumulation on the Greenland ice sheet from PARCA cores, J. Geophys. Res., 106(D24), 33839– 33851, https://doi.org/10.1029/2001JD900067, 2001.

Mosley-Thompson, E., Readinger, C. R., Craigmile, P., Thompson, L. G., and Calder, C. A.: Regional sensitivity of Greenland precipitation to NAO variability, Geophys. Res. Lett., 32, L24707, https://doi.org/10.1029/2005GL024776, 2005.

NEEM team: Eemian interglacial reconstructed from a greenland folded ice core, Nature, 493, 489–494, https://doi.org/10.1038/nature11789, 2013

705 Nerem, R.S., Beckley, B.D., Fasullo, J.T., Hamlington, B.D., Masters, D. and Mitchum, G.T.: Climate-change–driven accelerated sea-level rise detected in the altimeter era. Proceedings of the national academy of sciences, 115(9), pp.2022-2025, https://doi.org/10.1073/pnas.1717312115, 2018.

Noël, B., van de Berg, W. J., Lhermitte, S., and van den Broeke, M. R.: Rapid ablation zone expansion amplifies north Greenland mass loss, Science Advances, 5, eaaw0123, https://doi.org/10.1126/sciadv.aaw0123, 2019.

Oerlemans, J., and Vugts, H.F.: A Meteorological Experiment in the Melting Zone of the Greenland Ice Sheet. Bull. Amer.
710 Meteor. Soc., 74, 355–366, https://doi.org/10.1175/1520-0477(1993)074<0355:AMEITM>2.0.CO;2, 1993.

Ohmura, A., Steffen, K., Blatter, H., Greuell, W., Rotach, M., Konzelmann, T., Laternser, M., Abe-Ouchi, A. and Steiger, D.: Energy and mass balance during the melt season at the equilibrium line altitude, Paakitsoq, Greenland ice sheet. ETH Greenland Expedition Prog. Report no. 1, Dept of Geography, Swiss Fed. Inst, of Technol., Zurich, 1991.

Ohmura, A., Steffen, K., Blatter, H., Greuell, W., Rotach, M., Konzelmann,T., Forrer, J., Abe-Ouchi, A., Steiger.D., Stober,
715 M. and Niederbàumer, G.: Energy and mass balance during the melt season at the equilibrium line altitude, Paakitsoq, Greenland ice sheet. ETH Greenland Expedition Prog. Report no. 2, Dept of Geography, Swiss Fed. Inst, of Technol., Zurich, 1992.

Oksman, M., Kvorning, A. B., Larsen, S. H., Kjeldsen, K. K., Mankoff, K. D., Colgan, W., Andersen, T. J., Nørgaard-Pedersen, N., Seidenkrantz, M.-S., Mikkelsen, N., and Ribeiro, S.: Impact of freshwater runoff from the southwest
720 Greenland Ice Sheet on fjord productivity since the late 19th century, The Cryosphere, 16, 2471–2491, https://doi.org/10.5194/tc-16-2471-2022, 2022.

Olesen, O. B. and Braithwaite,R.J.: Field stations for glacier-climate research, West Greenland. In Oerlemans.]., ed. Glacier fluctuations and climatic change. Dordrecht, Kluwer Academic Publishers, 207-218, 1989.

Olesen, O., and Andreasen, J.-O: Glaciological, glacier-hydrological and climatological investigations around 66°N, West
725 Greenland. Rapport Grønlands Geologiske Undersøgelse, 115, 107–111. https://doi.org/10.34194/rapggu.v115.7842, 1983.

Picard, G., Dumont, M., Lamare, M., Tuzet, F., Larue, F., Pirazzini, R., and Arnaud, L.: Spectral albedo measurements over snow-covered slopes: theory and slope effect corrections, The Cryosphere, 14, 1497–1517, https://doi.org/10.5194/tc-14-1497-2020, 2020.

Reeh, N., Thompson, H. H., Higgins, A. K., Weidick, A. and Starzer, W..: Stability conditions of north-east Greenland
730 floating ice margins. In Climate change and sea level: final report of work undertaken for the Commission of the European Communities under contract No. ENV4−CT095−0124, 1 March 1996-28 February 1999 Copenhagen, Danish Polar Center. (Report 9.), 1999.

Reeh, N., O. B. Olesen, H. H. Thomsen, W. Starzer, and C. E. Bøggild, Mass balance parameterisation for Hans Tausen Iskappe, Peary Land, North Greenland, in The Hans Tausen Ice Cap. Glaciology and Glacial Geology, Meddelelser om
735 Grønland, vol. 39, edited by C. U. Hammer, pp. 57--69, Danish Polar Center, Museum Tusculanum Press, 2001.

Rignot, E., and Steffen, K.: Channelized bottom melting and stability of floating ice shelves, Geophys. Res. Lett., 35, L02503, https://doi.org/10.1029/2007GL031765, 2008.

Ridley, J. K., P. Huybrechts, J. M. Gregory, and J. A. Lowe: Elimination of the Greenland Ice Sheet in a High CO2 Climate. J. Climate, 18, 3409–3427, https://doi.org/10.1175/JCLI3482.1, 2005.

740   Reijmer, C., Kuipers Munneke, P., and Smeets, P.: Helheim firn aquifer weather station data and melt rates, Greenland, 2014–2016. Arctic Data Center. https://doi.org/10.18739/A26D5PB4R, 2019.

Samimi, S., Marshall, S.J., Vandecrux, B. and MacFerrin, M.: Time-domain reflectometry measurements and modeling of firn meltwater infiltration at DYE-2, Greenland. Journal of Geophysical Research: Earth Surface, 126(10), p.e2021JF006295, https://doi.org/10.1029/2021JF006295, 2021.

745   Sampson, K.: Shallow firn layer climatology derived from greenland climate network automatic weather station data. Master Thesis, Colorado University, https://doi.org/10.13140/RG.2.2.28475.90407, 2009.

Shuman, C. A., Steffen, K., Box, J. E., and Stearns, C. R.: A Dozen Years of Temperature Observations at the Summit: Central Greenland Automatic Weather Stations 1987–99, Journal of Applied Meteorology, 40(4), 741-752. Retrieved Jul 20, 2022, from https://journals.ametsoc.org/view/journals/apme/40/4/1520-0450_2001_040_0741_adyoto_2.0.co_2.xml, 2001.

750   Sigl, M., Winstrup, M., McConnell, J.R., Welten, K.C., Plunkett, G., Ludlow, F., Büntgen, U., Caffee, M., Chellman, N., Dahl-Jensen, D. and Fischer, H.: Timing and climate forcing of volcanic eruptions for the past 2,500 years, Nature, *523*(7562), pp.543-549, https://doi.org/10.1038/nature14565, 2015.

Simpson, C. J. W.: The British North Greenland Expedition, Geogr. J., 121, 274–289, https://doi.org/10.2307/1790892, 1955.

755   Steams, C. R., and G. A. Weidner, The polar automatic weather station project of the University of Wisconsin, in International Conference on the Role of the Polar Regions in Global Change: Proceedings of a conference held June 11-15, 1990, at the University of Alaska Fair- banks, vol. 1, edited by G. Weller et al., pp. 58-62, Geophysical Insti- tute, Univ. Alaska, Fairbanks AK, https://inis.iaea.org/collection/NCLCollectionStore/_Public/24/041/24041533.pdf?r=1, 1991.

Steffen, K.: Surface energy exchange at the equilibrium line on the Greenland ice sheet during onset of melt. Annals of
760   Glaciology, 21, 13-18. https://doi.org/10.3189/S0260305500015536, 1995.

Steffen, K., and deMaria, T.: Surface Energy Fluxes of Arctic Winter Sea Ice in Barrow Strait, Journal of Applied Meteorology and Climatology, 35(11), 2067-2079. Retrieved Feb 15, 2023, https://doi.org/10.1175/1520-0450(1996)035<2067:SEFOAW>2.0.CO;2, 1996.

Steffen, K., Box, J. E., and Abdalati, W.: Greenland climate network: GC-Net, in Glaciers, Ice Sheets and Volcanoes: A
765   Tribute to Mark F. Meier. Ed. S. Colbeck, US Army Cold Regions Reattach and Engineering (CRREL), CRREL Special Report, 98-103. URL, 1996.

Steffen, K., and Box, J.: Surface climatology of the Greenland Ice Sheet: Greenland Climate Network 1995–1999, J. Geophys. Res., 106(D24), 33951– 33964, https://doi.org/10.1029/2001JD900161, 2001.

Steffen, K., Cullen, N., Huff, R., Starkweather, S., Albert, T., and McAllister, M..: Variability and forcing of climate
770   parameters on the greenland ice sheet: greenland climate network (GC-NET), NASA Greenland Progress Report, PDF,
2003.

Steffen, K., Cullen, N. Huff, R., Maurer, J., Stober, M., Hepperle, J., and Heise, A.: Variability and forcing of climate
parameters on the greenland ice sheet: greenland climate network (GC-NET), NASA Greenland Progress Report, URL,
2005.

775   Steffen, K., Huff, R., Rial, J.: Greenland -accumulation and melt layers: regional climatology, process studies, and
seismicity, NASA Greenland Progress Report, PDF, 2006.

Steffen, K.; Vandecrux, B.; Houtz, D.; Abdalati, W.; Bayou, N.; Box, J.; Colgan, L.; Espona Pernas, L.; Griessinger, N.;
Haas-Artho, D.; Heilig, A.; Hubert, A.; Iosifescu Enescu, I.; Johnson-Amin, N.; Karlsson, N. B.; Kurup Buchholz, R.;
McGrath, D.; Cullen, N.J.; Naderpour, R.; Molotch, N.P.; Pederson, A. Ø.; Perren, B.; Philipps, T.; Plattner, G.K.; Proksch,
780   M.; Revheim, M. K.; Særrelse, M.; Schneebli, M.; Sampson, K.; Starkweather, S.; Steffen, S.; Stroeve, J.; Watler, B.;
Winton, Ø. A.; Zwally, J.; Ahlstrøm, A.: GC-Net Level 1 automated weather station data,
https://doi.org/10.22008/FK2/VVXGUT, GEUS Dataverse, V3, 2023.

Stroeve, J., Box, J.E., Wang, Z., Schaaf, C. and Barrett, A.: Re-evaluation of MODIS MCD43 Greenland albedo accuracy
and trends. Remote Sensing of Environment, 138, pp.199-214, https://doi.org/10.1016/j.rse.2013.07.023, 2013.

785   Thomas, R., Akins, T., Csatho, B., Fahnestock, M., Gogineni, P., Kim, C., Sonntag, J.: Mass Balance of the Greenland Ice
Sheet at High Elevations. Science, 289(5478):426-428. https://doi.org/10.1126/science.289.5478.426. 2000 .

Thomas, R. H.: Program for Arctic Regional Climate Assessment (PARCA): Goals, key findings, and future directions, J.
Geophys. Res., 106(D24), 33691– 33705, https://doi.org/10.1029/2001JD900042, 2001.

Thomsen, H. H., N. Reeh, O. B. Olesen, W. Starzer, and C. E. Bøggild, Bottom melting, surface mass balance and dynamics
790   of floating North-East Greenland ice tongues, Final report, EC Environment and Climate Programme 1994-1998,
Copenhagen, 1999

Toniazzo, T., Gregory, J.M., and P. Huybrechts, P.: Climatic Impact of a Greenland Deglaciation and Its Possible
Irreversibility. J. Climate, 17, 21–33, https://doi.org/10.1175/1520-0442(2004)017<0021:CIOAGD>2.0.CO;2, 2004.

Van As, D.: Warming, glacier melt and surface energy budget from weather station observations in the Melville Bay region
795   of northwest Greenland. Journal of Glaciology, 57(202), 208-220, https://doi.org/10.3189/002214311796405898, 2011.

Van As, D., Bøggild, C. E., Nielsen, S., Ahlstrøm, A. P., Fausto, R. S., Podlech, S., and Andersen, M. L.: Climatology and
ablation at the South Greenland ice sheet margin from automatic weather station observations, The Cryosphere Discuss., 3,
117–158, https://doi.org/10.5194/tcd-3-117-2009, 2009.

Van den Broeke, M.R., Duynkerke, P.G. and Oerlemans, J.: The observed katabatic flow at the edge of the Greenland ice
800   sheet during GIMEX-91. Global and Planetary Change, 9(1-2), pp.3-15. https://doi.org/10.1016/0921-8181(94)90003-5,
1994.

van den Broeke, M., D. van As, C. Reijmer, and R. van de Wal: Assessing and Improving the Quality of Unattended Radiation Observations in Antarctica. J. Atmos. Oceanic Technol., 21, 1417–1431, https://doi.org/10.1175/1520-0426(2004)021<1417:AAITQO>2.0.CO;2, 2004.

805 Vandecrux, B.: GC-Net evaluation scripts (Version v1). Zenodo. https://doi.org/10.5281/zenodo.7728938, 2023.

Vandecrux, B., Box, J., Houtz, D., and Revheim, M. K. The GC-Net level 1 dataset and processing scripts, https://github.com/GEUS-Glaciology-and-Climate/GC-Net-level-1-data-processing, Last access: 01-03-2023, 2023a.

Vandecrux, B., Houtz, D., Box, J.E.: GC-Net historical metadata compilation [Data set]. Zenodo, https://doi.org/10.5281/zenodo.7829106, 2023b.

810 Vandecrux, B. and Box, J.E.: GC-Net AWS observed and estimated positions (Version v1) [Data set]. Zenodo. https://doi.org/10.5281/zenodo.7729070, 2023c.

Van de Wal, R.S.W. and Russell, A.J.: A comparison of energy balance calculations, measured ablation and meltwater runoff near Søndre Strømfjord, West Greenland. Global and Planetary change, 9(1-2), pp.29-38. https://doi.org/10.1016/0921-8181(94)90005-1, 1994.

815 Wang, W., Zender, C. S., van As, D., Smeets, P. C. J. P., and van den Broeke, M. R.: A Retrospective, Iterative, Geometry-Based (RIGB) tilt-correction method for radiation observed by automatic weather stations on snow-covered surfaces: application to Greenland, The Cryosphere, 10, 727–741, https://doi.org/10.5194/tc-10-727-2016, 2016.

Weidner, G. A., and C. R. Steams, A Two-Year Record of the Climate on the Greenland Crest from an Automatic Weather Station, in International Conference on the Role of the Polar Regions in Global Change: Proceedings of a conference held 820 June 11-15, 1990, at the University of Alaska Fair- banks, vol. 1, edited by G. Weller et al., pp. 58-62, Geophysical Institute, Univ. Alaska, Fairbanks AK, 1991.

Weiser, U., Olefs, M., Schöner, W., Weyss, G., and Hynek, B.: Correction of broadband snow albedo measurements affected by unknown slope and sensor tilts, The Cryosphere, 10, 775–790, https://doi.org/10.5194/tc-10-775-2016, 2016.

Wilkinson, M., Dumontier, M., Aalbersberg, I. et al. The FAIR Guiding Principles for scientific data management and 825 stewardship. Sci Data 3, 160018. https://doi.org/10.1038/sdata.2016.18, 2016.

Zender, C., Wang, W., Laffin, M. and Saini, A.: JAWS: An extensible toolkit to harmonize and analyze polar automatic weather station datasets. University of California, Irvine. PDF https://github.com/jaws/jaws 2018.